

1 **IceChrono1: a probabilistic model to compute a common**
2 **and optimal chronology for several ice cores**

3

4 **F. Parrenin^{1,2}, L. Bazin³, E. Capron⁴ and A. Landais³, B. Lemieux-Dudon⁵, V.**
5 **Masson-Delmotte³**

6 [1]{CNRS, LGGE, F-38041 Grenoble, France}

7 [2]{Univ. Grenoble Alpes, LGGE, F-38041 Grenoble, France}

8 [3]{British Antarctic Survey, Madingley Road, High Cross, Cambridge, CB3 0ET, UK}

9 [4]{Institut Pierre-Simon Laplace/Laboratoire des Sciences du Climat et de l'Environnement,
10 UMR 8212, CEA-CNRS-UVSQ, 91191 Gif-sur-Yvette, France}

11 [5]{Laboratoire Jean Kuntzmann, Grenoble, France}

12 Correspondence to: F. Parrenin (parrenin@ujf-grenoble.fr)

13

14 **Abstract**

15 Polar ice cores provide exceptional archives of past environmental conditions. The dating of
16 ice cores and the estimation of the age scale uncertainty are essential to interpret the climate
17 and environmental records that they contain. It is however a complex problem which involves
18 different methods. Here, we present IceChrono1, a new probabilistic model integrating
19 various sources of chronological information to produce a common and optimized chronology
20 for several ice cores, as well as its uncertainty. IceChrono1 is based on the inversion of three
21 quantities: the surface accumulation rate, the Lock-In Depth (LID) of air bubbles and the
22 vertical thinning function. The chronological information integrated into the model are:
23 models of the sedimentation process (accumulation of snow, densification of snow into ice
24 and air trapping, ice flow), ice and air dated horizons, ice and air depth intervals with known
25 durations, Δ depth observations (depth shift between synchronous events recorded in the ice
26 and in the air) and finally air and ice stratigraphic links in between ice cores. The optimization
27 is formulated as a least squares problem, implying that all densities of probabilities are
28 assumed to be Gaussian. It is numerically solved using the Levenberg-Marquardt algorithm
29 and a numerical evaluation of the model's Jacobian. IceChrono follows an approach similar to

1 that of the Datice model which was recently used to produce the AICC2012 chronology for 4
2 Antarctic ice cores and 1 Greenland ice core. IceChrono1 provides improvements and
3 simplifications with respect to Datice from the mathematical, numerical and programming
4 point of views. The capabilities of IceChrono is demonstrated on a case study similar to the
5 AICC2012 dating experiment. We find results similar to those of Datice, within a few
6 centuries, which is a confirmation of both IceChrono and Datice codes. We also test new
7 functionalities with respect to the original version of Datice: observations as ice intervals with
8 known durations, correlated observations, observations as gas intervals with known durations
9 and observations as mix ice-air stratigraphic links. IceChrono1 is freely available under the
10 GPL v3 open source license.

11

12 **1 Introduction**

13 Polar ice cores provide continuous records of key past features of the climate and the
14 environment, with local, regional and global relevance (e.g., Ahmed et al., 2013; EPICA
15 community members, 2004; NorthGRIP project members, 2004; WAIS Divide Project
16 Members, 2013). Tracers of polar climate (e.g., Jouzel et al., 2007), ice sheet topography
17 (NEEM community Members, 2013), water cycle (Schoenemann et al., 2014; e.g., Stenni et
18 al., 2010; Winkler et al., 2012), aerosol deposition (e.g., Lambert et al., 2012; Wolff et al.,
19 2006) and global atmospheric composition (e.g., Ahn and Brook, 2014; Loulergue et al.,
20 2008; Marcott et al., 2014) measured in ice cores unveil sequences of events on seasonal to
21 glacial-interglacial time scales.

22 However, the prior to interpretation of polar ice core records is the complex task of building
23 two robust time-depth relationships, one for the tracers measured in the ice phase (e.g. water
24 isotopes, particulates and chemical impurities) and one for those measured in the air phase
25 (e.g. greenhouse gas concentration, isotopic composition of gases). The firn, where snow is
26 gradually compacted into ice, constitutes the upper 50-120 m part of ice sheets. The firn is
27 permeable and air is only locked-in at its base, at a depth level called the Lock-In Depth
28 (LID). As a result, the entrapped air is always younger than the surrounding ice at any depth
29 level. Through gravitational fractionation processes, LID is closely related to the isotopic
30 composition of $\delta^{15}\text{N}$ of N_2 in air bubbles data (e.g., Buizert et al., 2015; Goujon et al., 2003;
31 Parrenin et al., 2012a; Schwander et al., 1993). The temporal evolution of the age difference
32 between ice and air at a given depth must therefore be estimated using firn densification

1 modeling and air $\delta^{15}\text{N}$. This age difference is essential for clarifying the exact timing between
2 changes in atmospheric CO₂ concentration and Antarctic surface temperature during
3 deglaciations (Caillon et al., 2003; e.g., Landais et al., 2013; Monnin et al., 2001; Parrenin et
4 al., 2013; Pedro et al., 2011). However, glacial-interglacial Antarctic firn changes remain
5 poorly understood (e.g., Capron et al., 2013).

6 Several strategies have been developed to build ice and gas chronologies. We briefly describe
7 these methods, their strengths and caveats hereafter:

8 1) Annual layer counting (e.g., Rasmussen et al., 2006; WAIS Divide Project Members, 2013;
9 Winstrup et al., 2012). Only applicable when accumulation rates are sufficiently high to make
10 this annual layer identification possible, this method provides accurate estimates of event
11 durations and small uncertainties on the absolute age of the upper ice sections. However, the
12 cumulative nature of the errors, associated with the increasing number of counted layers, leads
13 to a decrease of the accuracy of absolute age with depth. For instance, the GICC05
14 (Greenland Ice Core Chronology 2005) composite timescale for Greenland ice cores
15 (Rasmussen et al., 2006; Seierstad et al., 2014; Svensson et al., 2008), is associated with a
16 maximum counting error of only 45 years at \sim 8.2 ka B1950 (Before 1950 C.E.). This error
17 increases progressively with depth, reaching more than 2500 years at \sim 60 ka B1950. Annual
18 layer counting techniques cannot be applied when the annual layer thickness is too small to be
19 resolved visually, e.g. in ice cores from central East Antarctica.

20 2) Use of absolute age markers in ice cores. Well-dated tephra layers identified in ice cores
21 during the last millennia provide precious constraints (e.g., Sigl et al., 2014). Beyond that
22 period, absolute age markers are very scarce. The links between ^{10}Be peaks and well-dated
23 magnetic events (Raisbeck et al., 2007) have provided an age marker for the Laschamp event
24 (Singer et al., 2009). Promising results have recently been obtained using radiochronologic
25 dating tools (Aciego et al., 2011; Buizert et al., 2014; Dunbar et al., 2008).

26 3) Orbital dating in ice cores. Because there are few absolute constraints in ice cores beyond
27 60 ka B1950 (limit for the layer counting in the NGRIP ice core), orbital tuning is the most
28 effective method to provide chronological constraints on ice core deepest sections. In the first
29 orbital dating exercises, tie points were determined from the tuning of water isotopic records
30 on insolation curves (e.g., Parrenin et al., 2004), which limits further investigations of polar
31 climate relationships with orbital forcing. More recent chronologies tried to circumvent this
32 assumption and focused on non-climatic orbital markers. Three complementary tracers are

1 currently used: the $\delta^{18}\text{O}$ of atmospheric O_2 ($\delta^{18}\text{O}_{\text{atm}}$) (e.g., Bender et al., 1994; Dreyfus et al.,
2 2007), $\delta\text{O}_2/\text{N}_2$ (e.g., Bender, 2002; Kawamura et al., 2007; Suwa and Bender, 2008) and the
3 total air content (e.g., Raynaud et al., 2007). While the link between $\delta^{18}\text{O}_{\text{atm}}$ and precession is
4 explained by variations in the water cycle of the low latitudes, relationships between $\delta\text{O}_2/\text{N}_2$,
5 air content and local summer insolation are understood to arise from changes in the surface
6 snow energy budget influencing its metamorphism. Without a precise understanding of
7 mechanisms linking these tracers to their respective orbital targets, the associated
8 uncertainties remain large, 6 ka for $\delta^{18}\text{O}_{\text{atm}}$ and 3 to 4 ka for $\delta\text{O}_2/\text{N}_2$ and air content (Bazin et
9 al., 2013, 2014; Landais et al., 2012).

10 4) Ice core record synchronization. Inter-ice core matching exercises are undertaken to
11 transfer absolute or orbital dating information from one ice core to another one. It generally
12 relies on the global synchronicity of changes in atmospheric composition (CO_2 , CH_4
13 concentration, and $\delta^{18}\text{O}_{\text{atm}}$) (Bender et al., 1994; Blunier and Brook, 2001; Monnin et al.,
14 2004), the identification of volcanic sulfate spikes within a given area (Parrenin et al., 2012b;
15 Severi et al., 2007) or the hypothesis of synchronous regional deposition of aerosols recorded
16 as ice impurities (Seierstad et al., 2014). In the first case, limitations are associated with the
17 smoothing of atmospheric composition changes through firn air diffusion. In the second case,
18 mismatches may arise through incorrect identification of events in different ice cores.

19 5) Correlation with other well-dated climatic records. In some cases, high-resolution calcite
20 $\delta^{18}\text{O}$ records and precise U/Th dates on speleothems have been used to adjust ice core
21 chronologies (Barker et al., 2011; Buizert et al., 2015; Parrenin et al., 2007a). Pinning ice core
22 and speleothem records is attractive to reduce absolute age uncertainties especially during
23 past abrupt climatic events of glacial periods. However, these exercises rely on the
24 assumption of simultaneous abrupt climatic changes recorded in ice core (e.g. water isotopes,
25 CH_4) and low latitudes speleothem $\delta^{18}\text{O}$ records (mostly reflecting changes in regional
26 atmospheric water cycle). A main limitation of this method lies in the validity of this
27 assumption.

28 6) Modeling of the sedimentation process: snow accumulation, snow densification into ice, air
29 bubbles trapping and ice flow (Goujon et al., 2003; Huybrechts et al., 2007; Johnsen et al.,
30 2001). Glaciological modeling provides a chronology derived from the estimate of the annual
31 layer thickness, and therefore, leads to more realistic event durations when the accumulation
32 history and thinning function are well constrained. A side product of glaciological modelling

1 is the quantification of changes in surface accumulation rates, and the quantification of the
2 initial geographical origin of ice. These additional informations are necessary to convert
3 measurements of concentrations of chemical species in ice cores into deposition fluxes, and to
4 correct ice core records from upstream origin effects (e.g., EPICA community members,
5 2006; Röthlisberger et al., 2008). Caveats are caused by unknown parameters of such
6 glaciological models, such as amplitude of accumulation change between glacial and
7 interglacial periods, the basal melting or the vertical velocity profile, which have a growing
8 influence at depth.

9 A common and optimal chronology for several ice cores can be built through the combination
10 of several of these methods in the frame of a probabilistic approach. The first attempts used
11 absolute and orbitally-tuned age markers along one ice core to constrain the unknown
12 parameters of an ice flow model (e.g., Parrenin et al., 2001, 2004; Petit et al., 1999). This
13 method had however several limitations. First, the uncertainties associated with the ice flow
14 model could not be taken into account, resulting in underestimated uncertainties. Second, the
15 stratigraphic links between ice cores were not exploited, each ice core was dated separately
16 resulting in inconsistent chronologies.

17 A new probabilistic approach based on a Bayesian framework was subsequently introduced.
18 The first tool, Datice, was developed by Lemieux-Dudon et al. (2010a, 2010b). It introduced
19 modeling errors on three canonical glaciological quantities of the dating problem: the
20 accumulation rate, the LID of air bubbles and the vertical thinning function (i.e. ratio between
21 the in-situ annual layer vertical thickness on its initial surface thickness). This method starts
22 from prior (also called “background”) scenario for the three glaciological parameters
23 corresponding to a prior chronology for each ice cores. These scenarios, deduced from a
24 modeling of the sedimentation process, are associated with an uncertainty related to the
25 degree of confidence in these prior scenarios. A minimization approach is then applied to find
26 the best compromise between the prior chronological information for each ice core as well as
27 absolute and relative age markers in the ice and in the air phases. This approach has been
28 validated through the Datice tool and applied to build the Antarctic Ice Cores Chronology
29 2012 (AICC2012), producing coherent ice and air timescales for five different ice cores
30 (Bazin et al., 2013; Veres et al., 2013): EPICA Dome C (EDC), Vostok (VK), Talos Dome
31 (TALDICE), EPICA Dronning Maul Land (EDML) and NorthGRIP (NGRIP). Further
32 developments of Datice were performed to incorporate additional dating constraints such as

1 the depth intervals with known durations and correlation of errors (Bazin et al., 2014). Datice
2 provides an excellent reference for this Bayesian approach. Still, because Datice has been
3 developed over a long term period with a continuous effort in calculation optimization
4 through methodological improvement, the final code is difficult to access for a non-expert and
5 cannot easily be used as a community tool. We thus identified the need for an open and user-
6 friendly program with a performance similar to Datice but that can be more easily used and
7 implemented by different users within the ice core community.

8 In this paper, we present a new probabilistic model, IceChrono_v1, based exactly on the same
9 approach as Datice but with improvements and simplifications in the mathematical, numerical
10 and programming aspects. We first detail the IceChrono methodology highlighting the
11 differences to Datice (Section 2). We then perform dating experiments described in section 3
12 using IceChrono1. We first replicate the AICC2012 experiment, and perform 4 additional
13 experiments to test new functionalities of IceChrono1. The results of these experiments are
14 discussed in section 4. We summarize our main findings in the conclusions, and describe
15 perspectives for future developments of IceChrono in section 5.

16 **2 Method**

17 Table 1 lists all symbols used to describe the IceChrono1 methodology.

18 **2.1 Method summary**

19 The true chronology of an ice core, i.e. the ice and air ages at any depth, is a function of three
20 variables (also functions of the depth): the initial accumulation rate (the accumulation rate
21 when and where the particle was at surface), the lock-in depth of the air and the vertical
22 thinning function (the ratio between the thickness of a layer in the ice core to the initial
23 accumulation rate). This is what we call the forward model. These variables are unknown, and
24 to find our optimal chronology we estimate them based on:

25

- Prior information about their values on each ice core;
- Chronological observations, such as (see Figure 1): the ice or air age at a certain
27 depth, the time elapsed between two depths, the synchronicity between two ice or air
28 depths within two different ice cores or the depth shift between synchronous ice and
29 air depths within the same ice core.

1 All these different types of information, mathematically described as probability density
 2 functions (PDF), are assumed to be independent and are combined using a Bayesian
 3 framework to obtain posterior estimates of the three input variables (accumulation, LID and
 4 thinning) and of the resulting chronologies. Uncertainties on the prior estimates and on the
 5 observations are further assumed to be Gaussian and the forward model is linearized, which
 6 allow to use the Levenberg-Marquardt (hereafter LM) algorithm (Levenberg, 1944;
 7 Marquardt, 1963) to solve this least-squares optimization problem. The philosophy of the
 8 method is similar to that of the Datice method (Lemieux-Dudon et al., 2010a, 2010b).

9 2.2 The forward model

10 For each ice core denoted by its index k , given three quantities (initial accumulation rate, air
 11 Lock-In Depth -LID- and vertical ice thinning function), the model computes at any depth z_k
 12 the age for the ice matrix χ_k (in years relative to the drilling date) and the age for the
 13 air/hydrates contained in the ice ψ_k (which, for simplicity, are assumed unique, we do not
 14 consider the age distributions due to gas diffusion and progressive lock-in with depth) using
 15 the following formulas:

$$\chi_k(z_k) = \int_0^{z_k} \frac{D_k(z'_k)}{a_k(z'_k) \tau_k(z'_k)} dz'_k, \quad (1)$$

$$\psi_k(z_k) = \chi_k(z_k - \Delta d(z_k)), \quad (2)$$

$$\int_{z_k - \Delta d_k(z_k)}^{z_k} \frac{D(z'_k)}{\tau(z'_k)} dz'_k \approx \int_0^{l_k(z_k) D_k^{\text{firm}}(z_k)} \frac{1}{\tau_k(z'^{\text{ie}}_k)} dz'^{\text{ie}}_k, \quad (3)$$

16 where z_k is the depth in the ice core (0 is the surface), D_k is the relative density of the material
 17 with respect to pure ice (treated as a known time series), a_k is the initial accumulation rate
 18 (expressed in m ice-equivalent per year), τ_k is the incompressible thinning function, Δd_k is the
 19 Δ depth (the depth shift between synchronous events in the ice and air phases, taken as
 20 dependent on the air depth, by convention), l_k is the LID (taken as dependent on the air depth,
 21 by convention), D_k^{firm} is the average relative density of the firn when depth z_k was at LID
 22 (treated as a known time series, in practice often assumed constant) and z'^{ie}_k is the ice
 23 equivalent depth:

$$z'^{\text{ie}}_k = \int_0^{z_k} D_k(z'_k) dz'_k. \quad (4)$$

1 Note that in our convention inherited from glaciology, accumulation a_k is expressed in ice-
2 equivalent per year and that the thinning function τ_k is expressed with respect to this ice-
3 equivalent accumulation rate, hence the appearance of D_k in equation (1). We used this
4 convention because most of the ice flow models, which give prior estimates on the thinning
5 function (see below), only consider pure ice, i.e. they assume the snow is instantaneously
6 densified into ice when it falls at the surface of the ice sheet.

7 The first equation integrates along the depth axis the number of annual layers per meter from
8 the surface. The second equation means that the air age at depth z_k is equal to the ice age at
9 depth $z_k - \Delta d_k$. This is the definition of Δ depth. The third equation means that if one virtually
10 un-thins a depth interval between an ice depth and the synchronous air depth, one gets the
11 Unthinned Lock-In Depth in Ice Equivalent (ULIDIE, see Figure 2). The right-hand side of
12 the second equation is an approximation, since we assume that the vertical thinning function
13 in the firn is constant through time. But the vertical thinning function being usually very close
14 to 1 in the firn, this assumption is almost verified. No other approximation is introduced in
15 this set of equations. However, there are additional approximations in the sedimentation
16 models that provide the values of a_k , l_k and τ_k and we will discuss the errors linked to these
17 approximations below.

18 Let us assume we have prior estimates of the accumulation (denoted a_k^b), of the LID (denoted
19 l_k^b) and of the vertical ice thinning function (denoted τ_k^b). The prior information can come
20 from a combination of models and data. Typically, ice flow models can give an estimate of the
21 vertical thinning function, ice δD and $\delta^{18}\text{O}$ are often used to deduced accumulation rates (e.g.,
22 Parrenin et al., 2007b), firn densification models or $\delta^{15}\text{N}$ measurements in air bubbles are used
23 to deduce the LID. We now define logarithmic corrections functions:

$$c_k^a = \ln(a_k/a_k^b), \quad (5)$$

$$c_k^l = \ln(l_k/l_k^b), \quad (6)$$

$$c_k^\tau = \ln(\tau_k/\tau_k^b), \quad (7)$$

24 so that the forward model effectively takes as inputs the three logarithmic correction functions
25 instead of the three raw glaciological quantities. This change of variable allows to transform
26 Jeffreys variables into Cartesian variables (Tarantola, 2005) so as to express our problem into
27 a least-squares problem and will allow us to reduce the number of variables to be inverted
28 (see below).

1 The three prior quantities a^b_k , l^b_k and τ^b_k as well as the relative density D_k are discretized onto
2 the same fine depth grid: $z_{k,i}$ (i being the index of the node), called the *age equation grid*,
3 which may not be regular. This allows us to compute prior ice and air age scales. Then, we
4 discretize the correction functions c^a_k , c^l_k and c^τ_k onto coarser grids, which also may not be
5 regular and which depend on the age for a and l and on the depth for τ : $t^a_{k,i}$, $t^l_{k,i}$, $z^\tau_{k,i}$ (i being the
6 index of the node). We note $C^a_k = (c^a_{k,i})_i$, $C^l_k = (c^l_{k,i})_i$ and $C^\tau_k = (c^\tau_{k,i})_i$ the correction vectors. These
7 grids are coarser than the age grid to limit the number of variables to be inverted. The
8 correction functions are then transferred to the age equation grid using a linear interpolation
9 (for a and l , this step requires to use the prior age scale). This allows us to compute the three
10 glaciological quantities a_k , l_k and τ_k onto the age equation grid. We write X the vector
11 containing all the correction vectors on the coarse grids for all the ice core sites (the *model*
12 *input variables vector*).

13 Equation (1) for the ice age is first solved. Then Equation (3) for the Δ depth is solved which
14 allows to deduce the air age from Equation (2). To solve Equation (3), we first integrate D_k/τ_k
15 from the surface down to every depth in the age equation grid, i.e. we have a correspondence
16 table between real depths and unthinned-ice-equivalent (UIE) depths. Then, for every air real
17 depth in the age equation grid, we obtain the air UIE depth from the correspondence table. We
18 then subtract the second member of Equation (3) to this air UIE depth to get the ice UIE
19 depth. Finally, we use the correspondence table to obtain the ice real depth and the Δ depth.
20 When we need to compute the ice age, air age or Δ depth at depths which are not nodes of the
21 age equation grid (for example when comparing the model with observations, see below), we
22 use a linear interpolation.

23 **2.3 The cost function**

24 In probabilistic terms, one combines different sources of information which are assumed to be
25 independent (the prior and the observations) and one looks for the most probable scenario, i.e.
26 the most probable X (Tarantola, 2005). In mathematical terms, it corresponds to multiplying
27 the probability density functions (PDF) of the prior and of the observations, the result of this
28 multiplication being called the *likelihood function* L . Here, we assumed the PDFs to be
29 independent multivariate Gaussian distributions. The posterior likelihood function L can
30 therefore be written as:

$$L = \exp\left(-\frac{1}{2} J\right) \quad (8)$$

1 where J , the *cost function*, is the sum of least-squares terms, each corresponding to an
 2 independent multivariate Gaussian PDF. Maximizing the likelihood function therefore
 3 corresponds to minimizing the cost function. In this case, we assume the information on each
 4 ice core and on each ice core pair to be independent. The cost function can therefore be
 5 written as a sum of terms:

$$J = \sum_k J_k + \sum_{k < m} J_{k,m}, \quad (9)$$

6 where J_k is the term related to ice core number k and $J_{k,m}$ is the term related to the ice core pair
 7 (k,m) .

8 J_k measures the misfit of the model with respect to the prior and the observations for ice core
 9 number k . It is written as the sum of independent terms:

$$J_k = J_k^a + J_k^l + J_k^\tau + J_k^{ih} + J_k^{ah} + J_k^{ii} + J_k^{ai} + J_k^{\Delta d}, \quad (10)$$

10 where J_k^a , J_k^l and J_k^τ are the prior terms for respectively a , l and τ , J_k^{ih} is linked to ice dated
 11 horizons, J_k^{ah} is linked to air dated horizons, J_k^{ii} is linked to ice intervals with known duration,
 12 J_k^{ai} is linked to air intervals with known duration and $J_k^{\Delta d}$ is linked to Δ depth observations.

13 $J_{k,m}$ measures the misfit of the model with respect to the stratigraphic links in between ice
 14 cores k and m . It is the sum of 4 independent terms:

$$J_{k,m} = J_{k,m}^{ii} + J_{k,m}^{aa} + J_{k,m}^{ia} + J_{k,m}^{ai}, \quad (11)$$

15 where $J_{k,m}^{ii}$ is linked to ice-ice stratigraphic links, $J_{k,m}^{aa}$ is linked to air-air stratigraphic links,
 16 $J_{k,m}^{ia}$ is linked to ice-air stratigraphic links and $J_{k,m}^{ai}$ is linked to air-ice stratigraphic links.

17 We first describe the prior terms:

$$J_k^a = (\mathbf{R}_k^a)^T (\mathbf{P}_k^a)^{-1} (\mathbf{R}_k^a), \quad (12)$$

$$J_k^l = (\mathbf{R}_k^l)^T (\mathbf{P}_k^l)^{-1} (\mathbf{R}_k^l) \quad (13)$$

$$J_k^\tau = (\mathbf{R}_k^\tau)^T (\mathbf{P}_k^\tau)^{-1} (\mathbf{R}_k^\tau) \quad (14)$$

18 where \mathbf{P}_k^a , \mathbf{P}_k^l , \mathbf{P}_k^τ are the correlation matrices of the prior and where \mathbf{R}_k^a , \mathbf{R}_k^l , \mathbf{R}_k^τ are the
 19 residual vectors:

$$\mathbf{R}_k^a = \left(\frac{c_{k,i}^a}{\sigma_{k,i}^a} \right)_i, \quad (15)$$

$$\mathbf{R}_k^l = \left(\frac{c_{k,i}^l}{\sigma_{k,i}^l} \right)_i, \quad (16)$$

$$\mathbf{R}_k^\tau = \left(\frac{c_{k,i}^\tau}{\sigma_{k,i}^\tau} \right)_i, \quad (17)$$

1 with $(\sigma_{k,i}^a)_i$, $(\sigma_{k,i}^l)_i$, $(\sigma_{k,i}^\tau)_i$ the standard deviations for respectively the prior accumulation, LID
 2 and vertical thinning function. These three terms J_k^a , J_k^l and J_k^τ bring the “glaciological
 3 constraints” of the problem given by the sedimentation models. For example, they ensure that
 4 the optimum values for a , l and τ will be close to the prior values and also that their rates of
 5 change with respect to depth will be close to the rates of change of the prior values. That
 6 means the model giving the prior scenario for the accumulation, the LID and the vertical
 7 thinning function should have a quantified error. The correlation matrices define the
 8 correlation of uncertainties of the correction functions at different depth levels or ages. In
 9 practice, the IceChrono code is flexible, and any standard deviation vector and correlation
 10 matrix can be prescribed.

11 The other terms of J_k are simply comparisons to observations, assumed independent:

$$\mathbf{R}^T \mathbf{P}^{-1} \mathbf{R} \quad (18)$$

$$\mathbf{R} = \left(\frac{m_i - o_i}{\sigma_i} \right)_i \quad (19)$$

12 where R is the residual vector, $(m_i)_i$ are the model realizations of the observations, $(o_i)_i$ are the
 13 observations, $(\sigma_i)_i$ are their standard deviations and \mathbf{P} is the their correlation matrix. These
 14 terms are given in more details in the Appendix. Again, the IceChrono model is flexible, and
 15 whatever standard deviation vectors and correlation matrices can be prescribed.

16 For J_k^{ih} and J_k^{ah} , one prescribes depth, age and standard deviation of ice and air dated horizons
 17 and the correlation matrix. For J_k^{ii} and J_k^{ai} , one prescribes the top depth, bottom depth,
 18 duration and standard deviation of ice and air intervals with known durations and the
 19 correlation matrix. For $J_k^{\Delta d}$, one prescribes air depth, Δ depth and standard deviation of Δ depth
 20 markers and the correlation matrix. For $J_{k,m}^{ii}$, $J_{k,m}^{aa}$, $J_{k,m}^{ia}$, $J_{k,m}^{ai}$, one prescribes the depth in the

1 first core, the depth in the second core and a standard deviation in years of ice-ice, air-air, ice-
2 air or air-ice stratigraphic links and the correlation matrix.
3 The determination of the standard deviation vectors and of the correlation matrices of the
4 prior (resp. the observations) can be a difficult problem which requires an in-depth analysis of
5 the methods used to determine the prior (resp. the observations).

6 **2.4 Optimization**

7 We now try to find the X input vector that minimizes the cost function defined in Equation
8 (9). This least-squares optimization problem is solved using a standard Levenberg-Marquardt
9 (LM) algorithm (Levenberg, 1944; Marquardt, 1963). The LM algorithm iteratively converges
10 toward a minimum of the cost function and stops when a convergence criteria is met. To
11 converge, the LM algorithm uses the Jacobian of the observation operator (the operator which
12 output all the residuals from the X vector), which is here calculated using a finite difference
13 approach. The LM algorithm gives as result the optimized values of the model input variables
14 vector \mathbf{X}^{opt} (containing the correction functions defined on the coarse grids) as well as an
15 approximate estimation of its *a posteriori* error covariance matrix \mathbf{C}^X : the algorithm
16 approximates the model by its linear tangent around the solution.
17 We write $\mathbf{G}(X)$ the forward model vector containing all the variables for which we want to
18 compute the optimal values and the uncertainties (in particular the ice and air ages on the age
19 equation grids). The optimal model is therefore $\mathbf{G}(X^{\text{opt}})$. From the model Jacobian \mathbf{G}' at X^{opt} ,
20 which is calculated using a numerical finite difference approach, and from \mathbf{C}^X , one can
21 compute an approximated value of the error covariance matrix for the model as:

$$\mathbf{C}^G \approx (\mathbf{G}') \mathbf{C}^X (\mathbf{G}')^T. \quad (20)$$

22 The diagonal elements of \mathbf{C}^G give the variance of the model's variables. In practice, the matrix
23 \mathbf{C}^G is never completely formed to limit the memory size of the program. Only diagonal bloc
24 elements corresponding to a particular variable (e.g., ice age) on a particular ice core are
25 calculated.
26 To ensure that the LM algorithm converges toward a global minimum of the cost function, we
27 initialize it with different initial conditions X_0 all taken randomly according to the prior
28 density of probability. We then check that the LM algorithm always converges toward the
29 same solution.

1 **2.5 Programming aspects**

2 IceChrono1 is entirely coded in the python v2 programming language. IceChrono1 both
3 resolves the optimization problem and provides figures to display the results. The core of the
4 code is entirely separated from the experiment set up directory which also contains the results
5 of the run and which is composed of: general parameter files, a directory for each ice core
6 (which contains the parameters and observations for the given ice core) and a directory for
7 each ice core pair (which contains the observations for the given ice core pair). Only a basic
8 understanding of python and an understanding of the structure of the experiment set up
9 directory are needed to run IceChrono1. A detailed tutorial on how to use the IceChrono1
10 software is also available within the code.

11 The core of the code is about 1000 lines long (including white lines and comments) and is
12 built using an object oriented paradigm. In such an object oriented language, apart for the
13 classical type of variables (integer, real, characters, etc.), one can define his own classes of
14 objects, containing variables and functions. In IceChrono1, a class exists for the ice core
15 objects. It contains the variables related to this ice core: the age equation grid, the correction
16 function grids, the prior scenarios and their associated standard deviations and correlation
17 matrices, the relative density profile, the correction functions, the observations and their
18 associated standard deviations and correlation matrices and the resulting calculated variables
19 (accumulation, LID and thinning, ice and air ages, Δ depth, ice and air layer thickness, etc.). It
20 also contains functions performing the following tasks: the initialization of the ice core (i.e.
21 reading of the parameters, priors and observations), the calculation of the age model, the
22 calculation of the residuals, the calculation of the forward model Jacobian, the calculation of
23 the standard deviations, the construction of the figures (for ice age, air age, accumulation,
24 LID, thinning, ice layer thickness and Δ depth) and the saving of the results. A class also exists
25 for the ice core pair objects. It contains all the stratigraphic links and their associated standard
26 deviation and correlation matrices relative to this ice core pair. It also contains functions that
27 perform the following tasks: the initialization of the ice core pair, the calculation of the
28 residuals, the construction of the figures (for ice-ice links, air-air links, ice-air links and air-ice
29 links). The main program is kept as simple and straightforward as possible.

30 We used the LM algorithm as implemented in the 'leastsq' function from the 'scipy.optimize'
31 library, which also provides an automatic convergence criteria. It does not try to minimize
32 directly the cost function, but rather a residual vector, the components of this residual vector

1 being supposed independent from each others and with a unit standard deviation. Inside each
2 term of the cost function:

$$\mathbf{R}^T \mathbf{P}^{-1} \mathbf{R} , \quad (21)$$

3 We allow defining a correlation matrix \mathbf{P} so that the residuals can actually be correlated. We
4 thus used a Cholesky decomposition of \mathbf{P} :

$$\mathbf{P} = \mathbf{P}^{1/2} \mathbf{P}^{1/2} , \quad (22)$$

5 and a change of variable:

$$\mathbf{R}' = (\mathbf{P}^{1/2})^{-1} \mathbf{R} , \quad (23)$$

6 to transform, the residual vector into a vector composed of independent variables with unit
7 standard deviation. The associated term of the cost function can now be written:

$$(\mathbf{R}')^T \mathbf{R}' , \quad (24)$$

8 that is, the residuals are now independent and with a unit standard deviation.

9 2.6 Availability

10 IceChrono1 is an open source model available under the General Public License v3. It is
11 hosted on the github facility (<https://github.com/parrenin/IceChrono>). A mailing list exists for
12 general support or discussions (<https://groups.google.com/forum/?hl=en#!forum/icechrono>).
13 The current code (version 1) is also available as a supplement of this manuscript.

14

15 3 Dating experiments

16 In this section, we describe the setups and the results of various dating experiments.

17 3.1 Standard AICC2012 experiment

18 IceChrono1 is similar in scope to the Datice model (Lemieux-Dudon et al., 2010a, 2010b).
19 Datice has been used to build AICC2012, the most recent official chronology for the 4
20 Antarctic ice cores EPICA Dome C (EDC), Vostok (VK), Talos Dome (TALDICE), EPICA
21 Dronning Maud Land (EDML) and the Greenland ice core NorthGRIP (NGRIP) (Bazin et al.,
22 2013; Veres et al., 2013). The AICC2012 experiment was based on a previous experiment
23 (Lemieux-Dudon et al., 2010a) on 3 Antarctic ice cores (EDC, VK, EDML) and one
24 Greenland ice core (NGRIP), but with updated chronological information. All chronological

1 informations are available in the supplementary material of Bazin et al. (2013) and Veres et al.
2 (2013). This experiment integrates orbital tuning constraints based on the $\delta^{18}\text{O}_{\text{atm}}$, O_2/N_2 and
3 air content records (Bazin et al., 2013, p.201; Dreyfus et al., 2007, 2008; Landais et al., 2012;
4 Lipenkov et al., 2011; Raynaud et al., 2007; Suwa and Bender, 2008), layer counting on
5 NGRIP back to 60 kyr B1950 (Svensson et al., 2008 and references therein), a tephra layer
6 (Narcisi et al., 2006) dated independently at 93.2 ± 4.4 kyr B1950 (Dunbar et al., 2008), the
7 Laschamp geomagnetic excursion at 40.65 ± 0.95 kyr B1950 (Singer et al., 2009) and the
8 Brunhes-Matuyama geomagnetic reversal at $\sim 780.3 \pm 10$ kyr B1950 and its precursor at
9 798.3 ± 10 kyr B1950 (Dreyfus et al., 2008) identified in the ^{10}Be records (Raisbeck et al.,
10 2006, 2007; Yiou et al., 1997), a Holocene ^{10}Be -dendrochronology tie point on Vostok at
11 7.18 ± 0.1 kyr B1950 (Bard et al., 1997; Raisbeck et al., 1998), Δ depth observations at NGRIP
12 obtained by comparing the $\delta^{18}\text{O}_{\text{ice}}$ and $\delta^{15}\text{N}$ records (Capron et al., 2010; Huber et al., 2006;
13 Landais et al., 2004, 2005), air synchronization tie points using the CH_4 records (Buiron et al.,
14 2011; Capron et al., 2010; Landais et al., 2006; Lemieux-Dudon et al., 2010a; Louergue et
15 al., 2007; Schilt et al., 2010; Schüpbach et al., 2011) and the $\delta^{18}\text{O}$ records (Bazin et al., 2013)
16 and ice synchronization tie points using the volcanic records (Parrenin et al., 2012b; Severi et
17 al., 2007, 2012; Svensson et al., 2013; Udisti et al., 2004; Vinther et al., 2013) and the ^{10}Be
18 records (Raisbeck et al., 2007).

19 In this AICC2012-VHR (AICC2012 Very High Resolution) experiment, IceChrono1 is tested
20 on the exact same set up, using the same observations and the same definition of the prior
21 information as Datice was used. Only one aspect is modified: in AICC2012, the prior
22 correlation matrices for the thinning function and LID are supposed to have an across-
23 diagonal Gaussian decrease in amplitude. This Gaussian shape leads to a too high correlation
24 for neighboring points. As a consequence, these matrices are numerically very difficult to
25 invert (with a poor conditional state). We therefore opt for correlation matrices with an across-
26 diagonal linear decrease in amplitude. We use regular grids with a time step of 1 kyr for the
27 accumulation and LID correction functions and with 1001 nodes for the thinning correction
28 functions. For the age equation grid, we use a step of 0.55 m for EDC, 1 m for VK, 1 m for
29 TALDICE, 1 m for EDML and 1 m for NGRIP.

30 The IceChrono1 AICC2012-VHR experiment results are provided as a supplementary
31 material. This also includes all the figures produced by the IceChrono1 model.

1 **3.2 Sensitivity test to resolution**

2 In this experiment AICC2012-V2HR (AICC2012 Very Very High Resolution) experiment, we
3 test the impact of the resolution of the correction functions on the results of the optimization.
4 We use exactly the same setup than for the AICC2012-VHR experiment, except for the
5 resolution of the correction functions which is twice higher: we use regular grids with a time
6 step of 0.5 kyr for the accumulation and LID correction functions and with 2001 nodes for the
7 thinning correction functions.

8 Figure 3 compares the AICC2012-V2HR and AICC2012-VHR experiments for the ice age.
9 The differences are minor and do not exceed 60 yr.

10 Figure 4 compares the resulting chronologies for the EDC ice core using the IceChrono1
11 (experiment AICC2012-V2HR) and Datice codes, as well as their uncertainties. Note that we
12 did not use the official AICC2012 uncertainties for the ice and air ages (Bazin et al., 2013;
13 Veres et al., 2013), but rather the raw uncertainties as calculated by the Datice code (L. Bazin,
14 personal communication). The difference in both chronologies is less than 200 yr for the last
15 600,000 years and less than 500 yr all along the record. The uncertainties also show
16 comparable shapes. We remark a few noticeable differences, though. There is a high
17 frequency noise in the air age difference, especially for the most recent periods. This is due to
18 the facts that the $\delta^{15}\text{N}$ data which are used to infer the LID contain high frequency variations
19 and that Datice use a higher resolution than IceChrono for these periods (1.65 m for EDC, 2
20 m for VK, 3 m for EDML, 1 m for TALDICE and 1 m for NGRIP). For the last 60 kyr, the
21 uncertainties are almost always smaller in Datice than in IceChrono for the ice and almost
22 always smaller in IceChrono than in Datice for the air ages. For example, between 15 and 60
23 kyr B1950, the uncertainty on the gas age often decreases below 1000 yr in IceChrono but
24 never does in Datice. Also, the uncertainties of Datice are also smaller in the ice phase than in
25 the air phase.

26 **3.3 Test experiment for ice intervals with known durations**

27 We now perform a simplified dating experiment to test the inclusion of ice intervals with
28 known durations. This is a new type of observation introduced in IceChrono, not available in
29 the initial version of Datice (Lemieux-Dudon et al., 2010a, 2010b) and not used in the
30 AICC2012 experiment. It has only recently been developed in Datice (Bazin et al., 2014).
31 This experiment is called “test-ice-intervals-with-known-durations”. The experiment only

1 contains the NGRIP ice core. The resolution chosen for the correction functions is 200 yr for
2 the accumulation and LID correction functions and 501 nodes for the thinning correction
3 function.

4 The prior accumulation is deduced directly from the deuterium content of the ice using an
5 exponential relationship:

$$a^b = a^0 \exp(8\beta \Delta \delta^{18}\text{O}), \quad (25)$$

6 where $a^0=0.256$ ice-m/yr and $\beta=0.0193$. The accumulation covariance matrix is defined by a
7 uniform variance value of 20% and with a correlation matrix with an across-diagonal linear
8 decrease of length of 4000 yr. The prior thinning is deduced using the so-called pseudo-steady
9 assumption (Parrenin et al., 2006):

$$\tau^b = (1-\mu)\omega + \mu, \quad (26)$$

10 with $\mu=11\%$ being the ratio between melting and accumulation assumed constant through
11 time and with ω being the flux-shape function (Parrenin and Hindmarsh, 2007), defined using
12 a Lliboutry analytical model (Lliboutry, 1979):

$$\omega = 1 - \frac{p+2}{p+1}(1-\zeta) + \frac{1}{p+1}(1-\zeta)^{p+2}, \quad (27)$$

13 with $p=-0.61$. The covariance matrix of the thinning function is defined as: a variance, which
14 is assumed linearly related to the ice-equivalent depth z^{ie} :

$$\sigma^{\tau} = k \frac{z^{ie}}{H^{ie}} \quad (28)$$

15 where H^{ie} is the ice-equivalent ice thickness and $k=0.5$. The value of a^0 , β , μ and p were
16 adjusted to obtain a good fit with the layer counted GICC05 (Svensson et al., 2008) age
17 markers sampled every 5 kyr along the core.

18 Here we include only one type of observations, ice intervals with known durations, which
19 result from the layer counted GICC05 chronology (Svensson et al., 2008 and references
20 therein) covering the last 60 kyr. This information is sampled every kyr. The standard
21 deviation of each observation on every 1 kyr interval is taken as half the variation of the
22 maximum counting error (MCE) on this interval. All observations are assumed independent,
23 i.e. the error on one 1 kyr interval is not correlated with the error on another 1 kyr interval.

1 The NGRIP ice age results of IceChrono on this optimization experiment are plotted on
2 Figure 6. As expected, the time scale is tightly constrained by the GICC05 ice intervals with
3 known durations observations down to 60 kyr. The uncertainty of the optimized time scale is
4 smaller than half the MCE: for example, at 60 kyr B1950, the uncertainty of the optimized
5 age scale is 230 yr while half the MCE is 1300 yr. This is because the MCE is cumulative
6 while the uncertainties of the 1 kyr long intervals with known durations are assumed to be
7 independent and thus tend to cancel out. Indeed, the squared standard deviation of the sum of
8 independent Gaussian variable is the sum of the squared standard deviation of each
9 independent Gaussian variable. Beyond 60 kyr, when there are no ice intervals constraints
10 anymore, the uncertainty of the optimized age scale then increases quickly to reach \sim 7 kyr at
11 the bottom of the core.

12 **3.4 Test experiment for correlated errors of observations**

13 We now perform a simplified dating experiment to test the inclusion of correlated
14 uncertainties. This is a new functionality in IceChrono with respect to the first version of
15 Datice (Lemieux-Dudon et al., 2010a, 2010b) and which has not been used in the AICC2012
16 experiment. It has only recently been developed in Datice (Bazin et al., 2014). This
17 experiment is called “test-ice-intervals-with-known-durations-with-correlation”. Again, this
18 experiment contains only the NGRIP ice core. The resolution chosen for the correction
19 functions is 200 yr for the accumulation and LID correction functions and 501 nodes for the
20 thinning correction function.

21 The prior information is exactly the same as the previous experiment. Only one type of
22 observations is included: ice intervals with known durations. Again, this information comes
23 from the layer counted time scale GICC05 (Svensson et al., 2008 and references therein) and
24 is sampled every kyr. The standard deviation of each observation on every 1 kyr interval is
25 taken as half the variation of the maximum counting error (MCE) on this interval. Contrary to
26 the previous experiment, the observations are not assumed independent: the correlation matrix
27 is assumed to contain ones on its diagonal and 0.5 outside of it.

28 The NGRIP ice age results of IceChrono1 on this optimization experiment are plotted on
29 Figure 7. As expected, the time scale is well constrained by the GICC05 intervals with known
30 durations observations down to 60 kyr and explodes beyond this age. Contrary to the previous
31 experiment, the uncertainties of the intervals with known durations do not cancel out since

1 they are correlated. Indeed, the standard deviation of the sum of completely dependent
2 Gaussian variable is the sum of the standard deviations of the completely dependent Gaussian
3 variables. As a consequence, the a posteriori uncertainty of the optimized time scale increases
4 to ~ 900 yr at 60 kyr, compared to a MCE equal to ~ 2600 yr at this age.

5 **3.5 Test experiment for air intervals with known durations**

6 We now perform a simplified dating experiment to test the inclusion of air intervals with
7 known durations, which is a new type of observation in IceChrono with respect to the first
8 version of Datice (Lemieux-Dudon et al., 2010a, 2010b), not used in AICC2012. This
9 experiment is called test-air-intervals-with-known-durations. The experiment contains only
10 the EDC ice core. The resolution chosen for the correction functions is 200 yr for the
11 accumulation and LID correction functions and 501 nodes for the thinning correction
12 function. We perform the dating experiment only down to a depth of 1400 m (age of ~ 100 kyr
13 B1950).

14 The prior information is the same than for the AICC2012-VHR experiment. We include
15 observations as air intervals with known durations. This information comes from the layer
16 counted time scale GICC05 of NGRIP (Svensson et al., 2008 and references therein) and is
17 transferred onto EDC through a NGRIP- $\delta^{18}\text{O}_{\text{ice}}$ / EDC-CH₄ synchronization. Each air dated
18 interval is defined by the onsets of DO events (including the Younger-Dryas/Preboreal
19 -YD/PB- transition) down to DO12 (~ 46.8 kyr B1950). The top and bottom depths of the air
20 intervals with known durations are directly taken from fast CH₄ transitions (Louergue et al.,
21 2007, Table 2). The durations of the air intervals with known durations are directly taken from
22 the GICC05 time scale (Svensson et al., 2008, Table 1). The standard deviation of each
23 interval observation is taken as half the maximum counting error (MCE) on this interval. The
24 observations are assumed uncorrelated: the correlation matrix is assumed to equal to the
25 identity matrix. We also add the GICC05 age of the CH₄ YD/PB transition as an air dated
26 horizon. This is equivalent to using an air interval from the LID to the CH₄ YD/PB transition
27 with known duration, but it is numerically more stable since the LID is not fixed during the
28 iterative optimization procedure.

29 The EDC air age results of IceChrono on this optimization experiment are plotted on Figure 8.
30 As expected, the time scale is well constrained by the GICC05 intervals with known durations
31 observations down to DO12 and explodes beyond this age. The uncertainty on the absolute

1 age also tends to increase inside intervals with known durations. This is expected since the
2 total duration of an interval is constrained, but inside this interval, only the prior information
3 constrains the variation of the age. This feature is more visible here than in the two previous
4 experiments because of the uncertainty on the LID which has a direct impact on the
5 uncertainty of the air age from Equation (2). By comparison, the uncertainty of the
6 accumulation rate only has an impact on the uncertainty of the derivative of the ice age from
7 Equation (1).

8 **3.6 Test experiment for the mix ice-air stratigraphic links**

9 We now perform a simplified dating experiment to test the inclusion of mix ice-air
10 stratigraphic links, which is a new type of observation in IceChrono with respect to the first
11 version of Datice (Lemieux-Dudon et al., 2010a, 2010b), not used in the AICC2012. This
12 experiment is called test-mix-strati. The experiment contains only the EDC and NGRIP ice
13 cores. The resolution chosen for the correction functions is 200 yr for the accumulation and
14 LID correction functions and 501 nodes for the thinning correction function. We perform the
15 dating experiment only down to a depth of 1400 m for the EDC ice core (age of ~100 kyr
16 B1950).

17 The prior information for both the NGRIP and EDC ice cores are the same than for the test-
18 ice-dated-intervals and test-air-dated-intervals experiments, respectively. Only one type of
19 observations is included: mix ice-air stratigraphic links. This information comes from the
20 synchronization of the EDC CH₄ record with the NGRIP $\delta^{18}\text{O}$ record. Each stratigraphic link
21 is the onset of one DO event (including the Younger-Dryas/Preboreal transition) down to
22 DO12 (~46.8 kyr B1950). The EDC CH₄ depths are taken from Loulergue et al. (2007, table
23 2). The NGRIP $\delta^{18}\text{O}$ depths are taken from Svensson et al. (2008, table 1). The standard
24 deviation of each observation is taken as 100 yr for simplicity. The observations are assumed
25 uncorrelated: the correlation matrix is assumed to be equal to the identity matrix.

26 The NGRIP air age vs EDC ice age results of IceChrono on this optimization experiment are
27 plotted on Figure 9. While the prior scenario is in poor agreement with stratigraphic
28 observations the optimized chronology agrees with the observations within their confidence
29 intervals.

1 **4 Discussion**

2 **4.1 Robustness to a change of resolution**

3 It is important to assess whether the formulation of IceChrono1 is robust to a change of
4 resolution: when the resolution increases, the simulations should converge toward a
5 meaningful result. IceChrono1 uses different two different types of grids to optimize the ice
6 cores age scales: the age equation grids and the correction function grids.

7 The age equation grids are used to solve Eqs (1), (2) and (3). Eq (2) is the value of the ice age
8 function at a given depth, so it is clearly robust to a change of resolution. Eqs (1) and (3) are
9 integrals and are therefore also robust to a change of resolution.

10 Concerning the correction functions grids, we made two test experiments with different
11 resolutions: AICC2012-VHR and AICC2012-V2HR. The fact that the AICC2012-VHR and
12 AICC2012-V2HR experiments agree well indicates that the formulation of the optimization
13 problem in IceChrono1 is robust to a change of resolution of the correction functions.

14 **4.2 IceChrono-Datice comparison on the AICC2012 experiment**

15 The fact that IceChrono1 and Datice agree fairly well on this AICC2012 experiment indicates
16 that both codes, which have been developed independently using different programming
17 languages and different numerical schemes, are correct. But one has to keep in mind that both
18 codes are based on the same main principles, so this is not a confirmation of these principles.

19 Concerning the differences in the posterior confidence intervals observed for the last 60 kyr,
20 we note that Datice use an approximated version of Eq. (3) and that some limitations
21 regarding the calculation of the uncertainties in Datice are known (see SOM, l. 280-289, of
22 Bazin et al., 2014). These limitations are not present in IceChrono1 and all the uncertainties
23 are calculated using the same formula (Equation (20)). Some limitations have been corrected
24 in a more recent version of Datice (Bazin et al., 2014). During the last glacial period, there are
25 many CH₄ Antarctica-NGRIP stratigraphic links with uncertainties of a few centuries. The
26 NGRIP chronology being tightly constrained to GICC05 within 50 yr, it is expected that the
27 gas age uncertainty at EDC sometimes decreases below 1000 yr during this time period. The
28 posterior uncertainty calculated by IceChrono is therefore consistent with the chronological
29 information used, in contradiction to that calculated by Datice.

1 **4.3 IceChrono new functionalities**

2 IceChrono1 has 4 new functionalities with respect to the initial Datice model (Lemieux-
3 Dudon et al., 2010a, 2010b):

4 • observations as ice intervals with known durations ;
5 • observations with correlated uncertainties ;
6 • observations as air intervals with known durations ;
7 • observations as mix ice-air stratigraphic links.

8 We performed several tests which indicate that these functionalities work correctly. Note that
9 the first two of these functionalities have also been implemented in a recent version of Datice
10 (Bazin et al., 2014). The observations of intervals with known durations will be useful for
11 future dating efforts to account for the layer counting information. This information is
12 generally correlated since counting errors on two different intervals using the same method
13 could be biased the same way. Mix ice-air stratigraphic observations will also be useful when
14 accounting for the Antarctica-CH₄/Greenland-δ¹⁸O synchronization links.

15 **4.4 IceChrono-Datice codes comparison**

16 Although IceChrono1 follows an approach similar to that of Datice, there are mathematical,
17 numerical and programming differences with the initial version of Datice (Lemieux-Dudon et
18 al., 2010a, 2010b) that we will detail below.

19 1) Datice does not solve equation (3) but an approximation of it:

$$\Delta d(z) = D^{\text{firm}}(z) \times l(z) \times \tau(z), \quad (29)$$

20 that is, τ is assumed constant between the synchronous ice and air depths.

21 2) There is only one depth grid per drilling in Datice while the correction functions in
22 IceChrono1 are discretized on different, coarser grids than the age equation grid. This allows
23 to reduce significantly the number of variables to be inverted and therefore to decrease the
24 computation time. These coarser grids were not necessary in Datice since the analytical
25 gradients already reduce the computation time.

1 3) Uncertainties are assumed Gaussian on Δ depth observations in IceChrono1 while they are
2 assumed log-normal in Datice. In practice, if the uncertainty on the Δ depth observation is
3 small in front of the value of the Δ depth observation, this should make little difference.

4 4) In IceChrono1, we allow for mix ice-air and air-ice stratigraphic links in between ice cores.
5 This is new with respect to Datice. A concrete example of the use of mix ice-air stratigraphic
6 links could be the synchronization of Dansgaard-Oeschger events recorded in the methane
7 records in Antarctica and in the ice isotope records in Greenland, as illustrated in the test-mix-
8 strati experiment. This is especially useful when methane records for some Greenland ice
9 cores are not yet available at sufficient resolution.

10 5) IceChrono1 allows for ice and air intervals with known durations. The functionality of ice
11 intervals with known durations has also recently been implemented in Datice (Bazin et al.,
12 2014) to take into account the information from layer counting. An example of the use of air
13 intervals with known durations could be the dating of one Antarctic ice core using its methane
14 record synchronized to the NGRIP ice isotopic record dated by layer counting.

15 6) IceChrono1 allows correlated errors in observations for every kind of observation, while
16 the original version of Datice does not allow correlated errors for observations (Bazin et al.,
17 2013; Lemieux-Dudon et al., 2010a, 2010b; Veres et al., 2013). Note however that a new
18 version of Datice implements this new functionality (Bazin et al., 2014).

19 7) In IceChrono1, the Jacobian of the model is computed numerically by a finite difference
20 approach while it is computed analytically in Datice. This Jacobian is needed by the
21 minimizer to find the optimal solution X^{opt} and its uncertainty \mathbf{C}^X . When the optimal solution
22 is found, it also allows to evaluate the uncertainty of the model \mathbf{C}^G through equation (20). In
23 Datice, analytical expressions of the Jacobian with respect to X have been derived and these
24 expressions are used to numerically compute the Jacobian for a particular X . In IceChrono,
25 each component of the X vector are alternatively perturbed and the forward model G is run to
26 evaluate how the model $G(X)$ is modified. In other words, the Jacobian is evaluated by a finite
27 difference approach. While a numerical computation of the Jacobian leads to a slower
28 computation time, it leads to a more flexible use of the model since if one modifies the
29 formulation of the cost function, one does not need to derive again analytical expressions for
30 the Jacobian, which is a complex task.

31 8) IceChrono1 is coded in a simple, flexible and straightforward way using the object-oriented
32 python language. It is very simple in IceChrono1 to modify the parameters of the problem,

1 e.g. the age equation grid and the correction vectors grids. By comparison, IceChrono1 is
2 about 1000 lines long (including the construction of the figures) while Datice is about 30,000
3 lines long of fortran code (without any figure construction). The reduction of the code length
4 in IceChrono is in particular due to: 1) the use of the python programming language, which
5 was not advanced enough at the time when the Datice code was developed, 2) the use of the
6 python leastsq function, which automatically calculate the gradient of the observation
7 operator and the posterior \mathbf{C}^x variance-covariance matrix and 3) the use of a numerical
8 gradient of the model \mathbf{G}' . Datice also implements posterior diagnostics of the data assimilation
9 system which make its code length larger (Bazin et al., 2014). The simplicity of IceChrono
10 will make it easy to add new functionalities to the code.

11 **4.5 Current limitations of IceChrono and possible perspectives**

12 IceChrono1 is already a useful tool to define a common and optimized chronology for several
13 ice cores all together. It however has several limitations that we will discuss below.

14 1) All uncertainties are assumed Gaussian. While the Gaussian probability density functions
15 are the most often encountered in Science, it is not always appropriate. For example, the
16 volcanic synchronization of ice cores (e.g., Parrenin et al., 2012b) is ambiguous: a volcanic
17 peak in one ice core can sometimes be synchronized to several other volcanic peaks in the
18 other ice core. IceChrono1 therefore assumes that the features recognition has been performed
19 without ambiguity and that the only uncertainty remaining is the exact match of the two
20 features within their durations.

21 2) The forward dating model is assumed to be “almost linear” in the plausible vicinity of the
22 solution. Further developments would be necessary to diagnose if this assumption is justified.

23 3) IceChrono1 is not appropriate for optimizing the chronology of many ice cores at a very
24 high resolution: the computation time would be too high, due to the numerical finite
25 differences approach to evaluate the Jacobian matrices. In practice this is not a problem as a
26 high resolution is only necessary for recent periods. If, in the future, the need for a more
27 efficient dating model appears, we could develop an analytical gradient for the forward
28 model, as it is done in the Datice software.

29 4) The age observations on different cores or on different ice cores pairs are not always
30 independent (because the dating methods are the same). We might allow in the future to take
31 into account correlation of observations in-between ice cores and ice cores pairs.

1 5) IceChrono1 requires the need for external sedimentation models to infer prior scenarios
2 and their uncertainties. In practice, these sedimentation models also need to be optimized
3 using age observations. In a next step, we will incorporate sedimentation models directly into
4 IceChrono. The uncertainties of these sedimentation models could be inferred automatically
5 by comparing them to the age observations.

6 6) The stratigraphic observations in-between the different ice cores need to be derived
7 externally and imported as stratigraphic observations into IceChrono1. This step also requires
8 some prior knowledge about the sedimentation process. Therefore, it would be best to
9 incorporate it directly into the IceChrono software. Automatic methods for ice core
10 synchronization would eliminate this step which is most of the time done visually, in a
11 subjective, fastidious and undocumented way.

12 7) The layer counting dating of ice core needs to be done externally and imported as intervals
13 with known durations observations into IceChrono1. Again, this step also requires prior
14 knowledge about the sedimentation process (e.g., the typical annual layer thickness).
15 Therefore, it would be best to incorporate it directly into the IceChrono software. An
16 automatic method for layer counting has already been proposed (Winstrup et al., 2012).

17 8) The definition of realistic prior correlation matrices is a difficult issue which will be dealt
18 with in details in future studies.

19 **5 Conclusions**

20 We have developed and made accessible a new open-source probabilistic model to produce a
21 common and optimized age scale for several ice cores, taking into account modeling and
22 observation information. The code is similar in scope to Datice but has mathematical,
23 numerical and programming differences: IceChrono1 is simpler to use, more flexible to
24 develop and more powerful than Datice, although it might be slower to run depending on the
25 resolution which is chosen. When compared onto an AICC2012-like experiment, IceChrono1
26 and Datice generally produces similar results, which is a confirmation of both codes but
27 which is not a confirmation of their principles which are identical. There are some differences
28 in the evaluation of AICC2012 uncertainties for the last glacial period and IceChrono appears
29 more consistent with the chronological information which have been used. We also tested 4
30 new features of IceChrono1 with respect to Datice: the use of ice intervals with known
31 duration, the use of correlated observations, the use of air intervals with known durations, and
32 the use mix ice-air stratigraphic links. Although primarily built for ice cores, IceChrono1

1 could well be used to date other paleoclimatic archives like marine cores, lake cores,
 2 speleothems, etc.

3 The flexibility of IceChrono now opens interesting perspectives: the allowance of inter-cores
 4 and inter-cores-couples correlation, the coupling with sedimentation models, the coupling
 5 with automatic synchronization methods, the coupling with automatic layer counting
 6 methods. These developments will be made available in future versions of IceChrono.

7 Acknowledgements

8 This work benefited from helpful comments by E. Wolff, T. Heaton, and two other
 9 anonymous reviewers. We also thank Florent Molliex, Delphine Tardif-Becquet, M.
 10 Sacchettini, M. Nodet et E. Blayo for helpful exchanges. This work was funded by the
 11 INSU/LEFE project IceChrono and by the ANR project ADAGe.

12 Appendix

13 Below we describe in details the terms of the cost function which are linked to observations.

$$j_k^{\text{ih}} = (\mathbf{R}_k^{\text{ih}})^T (\mathbf{P}_k^{\text{ih}})^{-1} \mathbf{R}_k^{\text{ih}}, \quad (30)$$

$$\mathbf{R}_k^{\text{ih}} = \left(\frac{\chi_k^{\text{d}}(z_{k,i}^{\text{ih}}) - \chi_{k,i}^{\text{obs}}}{\sigma_{k,i}^{\text{ih}}} \right)_i, \quad (31)$$

14 where $z_{k,i}^{\text{ih}}$ is the depth of the i^{th} ice dated horizon in the k^{th} ice core, $\chi_{k,i}^{\text{obs}}$ is its age, $\sigma_{k,i}^{\text{ih}}$ is its
 15 standard deviation and where \mathbf{P}_k^{ih} is the correlation matrix.

$$j_k^{\text{ah}} = (\mathbf{R}_k^{\text{ah}})^T (\mathbf{P}_k^{\text{ah}})^{-1} \mathbf{R}_k^{\text{ah}}, \quad (32)$$

$$\mathbf{R}_k^{\text{ah}} = \left(\frac{\psi_k^{\text{d}}(z_{k,i}^{\text{ah}}) - \psi_{k,i}^{\text{obs}}}{\sigma_{k,i}^{\text{ah}}} \right)_i, \quad (33)$$

16 where $z_{k,i}^{\text{ah}}$ is the depth of the i^{th} air dated horizon in the k^{th} ice core, $\psi_{k,i}^{\text{obs}}$ is its age, $\sigma_{k,i}^{\text{ah}}$ is its
 17 standard deviation and where \mathbf{P}_k^{ah} is the correlation matrix.

$$j_k^{\text{ii}} = (\mathbf{R}_k^{\text{ii}})^T (\mathbf{P}_k^{\text{ii}})^{-1} \mathbf{R}_k^{\text{ii}}, \quad (34)$$

$$\mathbf{R}_k^{\text{ii}} = \left(\frac{\chi_k^{\text{d}}(z_{k,i}^{\text{ii,b}}) - \chi_k^{\text{d}}(z_{k,i}^{\text{ii,t}}) - \Delta \chi_{k,i}^{\text{obs}}}{\sigma_{k,i}^{\text{ii}}} \right)_i, \quad (35)$$

1 where $z^{ii,t}_{k,i}$ and $z^{ii,b}_{k,i}$ are the top and bottom depths of the i^{th} ice dated interval in the k^{th} ice
 2 core, $\Delta\chi^{\text{obs}}_{k,i}$ is its duration, $\sigma^{ii}_{k,i}$ is its standard deviation and where \mathbf{P}^{ii}_k is the correlation
 3 matrix.

$$j_k^{\text{ai}} = (\mathbf{R}_k^{\text{ai}})^T (\mathbf{P}_k^{\text{ai}})^{-1} \mathbf{R}_k^{\text{ai}}, \quad (36)$$

$$\mathbf{R}_k^{\text{ai}} = \left(\frac{\psi_k^{\text{d}}(z_{k,i}^{\text{ai,b}}) - \psi_k^{\text{d}}(z_{k,i}^{\text{ai,t}}) - \Delta\psi_{k,i}^{\text{obs}}}{\sigma_{k,i}^{\text{ai}}} \right)_i, \quad (37)$$

4 where $z^{\text{ai,t}}_{k,i}$ and $z^{\text{ai,b}}_{k,i}$ are the top and bottom depths of the i^{th} air dated interval in the k^{th} ice
 5 core, $\Delta\psi^{\text{obs}}_{k,i}$ is its duration, $\sigma^{\text{ii}}_{k,i}$ is its standard deviation and where \mathbf{P}^{ai}_k is the correlation
 6 matrix.

$$j_k^{\Delta d} = (\mathbf{R}_k^{\Delta d})^T (\mathbf{P}_k^{\Delta d})^{-1} \mathbf{R}_k^{\Delta d}, \quad (38)$$

$$\mathbf{R}_k^{\Delta d} = \left(\frac{\Delta d_k^{\text{d}}(z_{k,i}^{\Delta d}) - \Delta d_{k,i}^{\text{obs}}}{\sigma_{k,i}^{\Delta d}} \right)_i, \quad (39)$$

7 where $z^{\Delta d}_{k,i}$ is the depth of the i^{th} Δ depth observation in the k^{th} ice core, $\Delta d^{\text{obs}}_{k,i}$ is its observed
 8 value, $\sigma^{\Delta d}_{k,i}$ is its standard deviation and where $\mathbf{P}^{\Delta d}_k$ is the correlation matrix.

$$j_{k,m}^{\text{ii}} = (\mathbf{R}_{k,m}^{\text{ii}})^T (\mathbf{P}_{k,m}^{\text{ii}})^{-1} \mathbf{R}_{k,m}^{\text{ii}}, \quad (40)$$

$$\mathbf{R}_{k,m}^{\text{ii}} = \left(\frac{\chi_k^{\text{d}}(z_{k,m,i}^{\text{ii},1}) - \chi_m^{\text{d}}(z_{k,m,i}^{\text{ii},2})}{\sigma_{k,m,i}^{\text{ii}}} \right)_i, \quad (41)$$

9 where $z^{\text{ii},1}_{k,m,i}$ and $z^{\text{ii},2}_{k,m,i}$ are the depths in the k^{th} and m^{th} ice cores of the i^{th} ice-ice stratigraphic
 10 link in the (k,m) couple of ice cores, $\sigma^{\text{ii}}_{k,m,i}$ is its standard deviation and where $\mathbf{P}^{\text{ii}}_{k,m}$ is the
 11 correlation matrix.

$$j_{k,m}^{\text{aa}} = (\mathbf{R}_{k,m}^{\text{aa}})^T (\mathbf{P}_{k,m}^{\text{aa}})^{-1} \mathbf{R}_{k,m}^{\text{aa}}, \quad (42)$$

$$\mathbf{R}_{k,m}^{\text{aa}} = \left(\frac{\psi_k^{\text{d}}(z_{k,m,i}^{\text{aa},1}) - \psi_m^{\text{d}}(z_{k,m,i}^{\text{aa},2})}{\sigma_{k,m,i}^{\text{aa}}} \right)_i, \quad (43)$$

12 where $z^{\text{aa},1}_{k,m,i}$ and $z^{\text{aa},2}_{k,m,i}$ are the depths in the k^{th} and m^{th} ice cores of the i^{th} air-air stratigraphic
 13 link in the (k,m) couple of ice cores, $\sigma^{\text{aa}}_{k,m,i}$ is its standard deviation and where $\mathbf{P}^{\text{aa}}_{k,m}$ is the
 14 correlation matrix.

$$j_{k,m}^{\text{ia}} = (\mathbf{R}_{k,m}^{\text{ia}})^T (\mathbf{P}_{k,m}^{\text{ia}})^{-1} \mathbf{R}_{k,m}^{\text{ia}}, \quad (44)$$

$$\mathbf{R}_{k,m}^{\text{ia}} = \left(\frac{\chi_k^{\text{d}}(z_{k,m,i}^{\text{ia},1}) - \psi_m^{\text{d}}(z_{k,m,i}^{\text{ia},2})}{\sigma_{k,m,i}^{\text{ia}}} \right)_i, \quad (45)$$

1 where $z_{k,m,i}^{\text{ia},1}$ and $z_{k,m,i}^{\text{ia},2}$ are the depths in the k^{th} and m^{th} ice cores of the i^{th} ice-air stratigraphic
2 link in the (k,m) couple of ice cores, $\sigma_{k,m,i}^{\text{ia}}$ is its standard deviation and where $\mathbf{P}_{k,m}^{\text{ia}}$ is the
3 correlation matrix.

$$j_{k,m}^{\text{ai}} = (\mathbf{R}_{k,m}^{\text{ai}})^T (\mathbf{P}_{k,m}^{\text{ai}})^{-1} \mathbf{R}_{k,m}^{\text{ai}}, \quad (46)$$

$$\mathbf{R}_{k,m}^{\text{ai}} = \left(\frac{\psi_k^{\text{d}}(z_{k,m,i}^{\text{ai},1}) - \chi_m^{\text{d}}(z_{k,m,i}^{\text{ai},2})}{\sigma_{k,m,i}^{\text{ai}}} \right)_i, \quad (47)$$

4 where $z_{k,m,i}^{\text{ai},1}$ and $z_{k,m,i}^{\text{ai},2}$ are the depths in the k^{th} and m^{th} ice cores of the i^{th} air-ice stratigraphic
5 link in the (k,m) couple of ice cores, $\sigma_{k,m,i}^{\text{ai}}$ is its standard deviation and where $\mathbf{P}_{k,m}^{\text{ai}}$ is the
6 correlation matrix.

1 References

Aciego, S., Bourdon, B., Schwander, J., Baur, H. and Forieri, A.: Toward a radiometric ice clock: uranium ages of the Dome C ice core, *Quat. Sci. Rev.*, 30(19), 2389–2397, 2011.

Ahmed, M., Krusic, P. J., Charpentier Ljungqvist, F., Zorita, E. and others: Continental-scale temperature variability during the past two millennia, *Nat. Geosci.*, 6(5), 339–346, 2013.

Ahn, J. and Brook, E. J.: Siple Dome ice reveals two modes of millennial CO₂ change during the last ice age, *Nat. Commun.*, 5 [online] Available from: <http://www.nature.com/ncomms/2014/140429/ncomms4723/full/ncomms4723.html?message-global=remove> (Accessed 24 February 2015), 2014.

Bard, E., Raisbeck, G. M., Yiou, F. and Jouzel, J.: Solar modulation of cosmogenic nuclide production over the last millennium: comparison between ¹⁴C and ¹⁰Be records, *Earth Planet Sci Lett*, 150, 453–462, 1997.

Barker, S., Knorr, G., Edwards, R. L., Parrenin, F., Putnam, A. E., Skinner, L. C., Wolff, E. and Ziegler, M.: 800,000 Years of Abrupt Climate Variability, *Science*, 334(6054), 347–351, doi:10.1126/science.1203580, 2011.

Bazin, L., Landais, A., Lemieux-Dudon, B., Toyé Mahamadou Kele, H., Veres, D., Parrenin, F., Martinerie, P., Ritz, C., Capron, E., Lipenkov, V., Loutre, M.-F., Raynaud, D., Vinther, B., Svensson, A., Rasmussen, S. O., Severi, M., Blunier, T., Leuenberger, M., Fischer, H., Masson-Delmotte, V., Chappellaz, J. and Wolff, E.: An optimized multi-proxy, multi-site Antarctic ice and gas orbital chronology (AICC2012): 120–800 ka, *Clim Past*, 9(4), 1715–1731, doi:10.5194/cp-9-1715-2013, 2013.

Bazin, L., Lemieux-Dudon, B., Landais, A., Guillevic, M., Kindler, P., Parrenin, F. and Martinerie, P.: Optimisation of glaciological parameters for ice core chronology by implementing counted layers between identified depth levels, *Clim Past Discuss*, 10(4), 3585–3616, doi:10.5194/cpd-10-3585-2014, 2014.

Bender, M. L.: Orbital tuning chronology for the Vostok climate record supported by trapped gas composition, *Earth Planet Sci Lett*, 204, 275–289, 2002.

Bender, M., Sowers, T., Dickson, M. L., Orchado, J., Grootes, P., Mayewski, P. A. and Meese, D. A.: Climate connection between Greenland and Antarctica during the last 100,000 years, *Nature*, 372, 663–666, 1994.

Blunier, T. and Brook, E. J.: Timing of millennial-scale climate change in Antarctica and Greenland during the last glacial period, *Science*, 291(5501), 109–112, 2001.

Buiron, D., Chappellaz, J., Stenni, B., Frezzotti, M., Baumgartner, M., Capron, E., Landais, A., Lemieux-Dudon, B., Masson-Delmotte, V., Montagnat, M., Parrenin, F. and Schilt, A.: TALDICE-1 age scale of the Talos Dome deep ice core, East Antarctica, *Clim Past*, 7(1), 1–16, doi:10.5194/cp-7-1-2011, 2011.

Buizert, C., Baggenstos, D., Jiang, W., Purtschert, R., Petrenko, V. V., Lu, Z.-T., Müller, P., Kuhl, T., Lee, J., Severinghaus, J. P. and others: Radiometric ^{81}Kr dating identifies 120,000-year-old ice at Taylor Glacier, Antarctica, *Proc. Natl. Acad. Sci.*, 111(19), 6876–6881, 2014.

Buizert, C., Cuffey, K. M., Severinghaus, J. P., Baggenstos, D., Fudge, T. J., Steig, E. J., Markle, B. R., Winstrup, M., Rhodes, R. H., Brook, E. J. and others: The WAIS Divide deep ice core WD2014 chronology—Part 1: Methane synchronization (68–31 ka BP) and the gas age–ice age difference, *Clim. Past*, 11(2), 153–173, 2015.

Caillon, N., Severinghaus, J. P., Jouzel, J., Barnola, J.-M., Kang, J. and Lipenkov, V. Y.: Timing of Atmospheric CO_2 and Antarctic Temperature Changes Across Termination III, *Science*, 299(5613), 1728–1731, doi:10.1126/science.1078758, 2003.

Capron, E., Landais, A., Biron, D., Cauquoin, A., Chappellaz, J., Debret, M., Jouzel, J., Leuenberger, M., Martinerie, P. and Masson-Delmotte, V.: Glacial–interglacial dynamics of Antarctic firn columns: comparison between simulations and ice core air- δ ^{15}N measurements, *Clim. Past*, 9(3), 983–999, 2013.

Capron, E., Landais, A., Lemieux-Dudon, B., Schilt, A., Masson-Delmotte, V., Biron, D., Chappellaz, J., Dahl-Jensen, D., Johnsen, S., Leuenberger, M., Louergue, L. and Oerter, H.: Synchronising EDML and NorthGRIP ice cores using $\delta^{18}\text{O}$ of atmospheric oxygen ($\delta^{18}\text{O}_{\text{atm}}$) and CH_4 measurements over MIS5 (80–123 kyr), *Quat Sci Rev*, 29(1–2), 222–234, doi:DOI: 10.1016/j.quascirev.2009.07.014, 2010.

Dreyfus, G. B., Parrenin, F., Lemieux-Dudon, B., Durand, G., Masson-Delmotte, V., Jouzel, J., Barnola, J.-M., Panno, L., Spahni, R., Tisserand, A., Siegenthaler, U. and Leuenberger, M.: Anomalous flow below 2700 m in the EPICA Dome C ice core detected using $\delta^{18}\text{O}$ of atmospheric oxygen measurements, *Clim. Past*, 3(2), 341–353, doi:10.5194/cp-3-341-2007, 2007.

Dreyfus, G. B., Raisbeck, G. M., Parrenin, F., Jouzel, J., Guyodo, Y., Nomade, S. and Mazaud, A.: An ice core perspective on the age of the Matuyama–Brunhes boundary, *Earth Planet Sci Let*, 274(1–2), 151–156, doi:DOI: 10.1016/j.epsl.2008.07.008, 2008.

Dunbar, N. W., McIntosh, W. C. and Esser, R. P.: Physical setting and tephrochronology of the summit caldera ice record at Mount Moulton, West Antarctica, *Geol. Soc. Am. Bull.*, 120(7–8), 796–812, 2008.

EPICA community members: 8 glacial cycles from an Antarctic ice core, *Nature*, 429, 623–628, 2004.

EPICA community members: One-to-one coupling of glacial climate variability in Greenland and Antarctica, *Nature*, 444, 195–198, 2006.

Goujon, C., Barnola, J.-M. and Ritz, C.: Modeling the densification of polar firn including heat diffusion: application to close-off characteristics and gas isotopic fractionation for Antarctica and Greenland sites, *J. Geophys. Res.*, 108(D24), ACL10/1–10, doi:10.1029/2002JD003319, 2003.

Huber, C., Leuenberger, M., Spahni, R., Flückiger, J., Schwander, J., Stocker, T. F., Johnsen, S., Landais, A. and Jouzel, J.: Isotope calibrated Greenland temperature record over Marine

Isotope Stage 3 and its relation to CH₄, *Earth Planet Sci Let*, 243(3-4), 504–519, doi:DOI: 10.1016/j.epsl.2006.01.002, 2006.

Huybrechts, P., Rybak, O., Pattyn, F., Ruth, U. and Steinhage, D.: Ice thinning, upstream advection, and non-climatic biases for the upper 89% of the EDML ice core from a nested model of the Antarctic ice sheet, *Clim Past*, 3(4), 577–589, 2007.

Johnsen, S. J., Dahl-Jensen, D., Gundestrup, N., Steffensen, J. P., Clausen, H. B., Miller, H., Masson-Delmotte, V., Sveinbjornsdottir, A. E. and White, J.: Oxygen isotope and palaeotemperature records from six Greenland ice-core stations: Camp Century, Dye-3, GRIP, GISP2, Renland and NorthGRIP, *J Quat Sci*, 16, 299–307, 2001.

Jouzel, J., Masson-Delmotte, V., Cattani, O., Dreyfus, G., Falourd, S., Hoffmann, G., Minster, B., Nouet, J., Barnola, J. M., Chappellaz, J., Fischer, H., Gallet, J. C., Johnsen, S., Leuenberger, M., Louergue, L., Lüthi, D., Oerter, H., Parrenin, F., Raisbeck, G., Raynaud, D., Schilt, A., Schwander, J., Selmo, E., Souchez, R., Spahni, R., Stauffer, B., Steffensen, J. P., Stenni, B., Stocker, T. F., Tison, J. L., Werner, M. and Wolff, E. W.: Orbital and Millennial Antarctic Climate Variability over the Past 800,000 Years, *Science*, 317(5839), 793–796, doi:10.1126/science.1141038, 2007.

Kawamura, K., Parrenin, F., Uemura, R., Vimeux, F., Severinghaus, J. P., Matsumoto, K., Nakata, H., Nakazawa, T., Aoki, S., Jouzel, J., Fujii, Y. and Watanabe, O.: Northern Hemisphere forcing of climatic cycles over the past 360,000 years implied by absolute dating of Antarctic ice cores, *Nature*, 448, 912–917, doi:10.1038/nature06015, 2007.

Lambert, F., Bigler, M., Steffensen, J. P., Hutterli, M. and Fischer, H.: Centennial mineral dust variability in high-resolution ice core data from Dome C, Antarctica, *Clim Past*, 8(2), 609–623, doi:10.5194/cp-8-609-2012, 2012.

Landais, A., Barnola, J. M., Masson-Delmotte, V., Jouzel, J., Chappellaz, J., Caillon, N., Huber, C., Leuenberger, M. and Johnsen, S. J.: A continuous record of temperature evolution over a sequence of Dansgaard-Oeschger events during Marine Isotopic Stage 4 (76 to 62 kyr BP), *Geophys. Res. Lett.*, 31(22) [online] Available from: <http://onlinelibrary.wiley.com/doi/10.1029/2004GL021193/full> (Accessed 14 January 2015), 2004.

Landais, A., Dreyfus, G., Capron, E., Jouzel, J., Masson-Delmotte, V., Roche, D. M., Prié, F., Caillon, N., Chappellaz, J., Leuenberger, M., Lourantou, A., Parrenin, F., Raynaud, D. and Teste, G.: Two-phase change in CO₂, Antarctic temperature and global climate during Termination II, *Nat. Geosci.*, 6(12), 1062–1065, doi:10.1038/ngeo1985, 2013.

Landais, A., Dreyfus, G., Capron, E., Pol, K., Loutre, M. F., Raynaud, D., Lipenkov, V. Y., Arnaud, L., Masson-Delmotte, V., Paillard, D., Jouzel, J. and Leuenberger, M.: Towards orbital dating of the EPICA Dome C ice core using $\delta\text{O}_2/\text{N}_2$, *Clim Past*, 8(1), 191–203, doi:10.5194/cp-8-191-2012, 2012.

Landais, A., Jouzel, J., Masson-Delmotte, V. and Caillon, N.: Large temperature variations over rapid climatic events in Greenland: a method based on air isotopic measurements, *Comptes Rendus Geosci.*, 337(10), 947–956, 2005.

Landais, A., Waelbroeck, C. and Masson-Delmotte, V.: On the limits of Antarctic and marine climate records synchronization: Lag estimates during marine isotopic stages 5d and 5c, *Paleoceanography*, 21(1), PA1001, doi:10.1029/2005PA001171, 2006.

Lemieux-Dudon, B., Blayo, Petit, J. R. E., Waelbroeck, C., Svensson, A., Ritz, C., Barnola, J.-M., Narcisi, B. M. and Parrenin, F.: Consistent dating for Antarctica and Greenland ice cores, *Quat Sci Rev*, 29(1-2), 8–20, 2010a.

Lemieux-Dudon, B., Parrenin, F. and Blayo, E.: A Probabilistic Method to Construct an Optimal Ice Chronology for Ice Cores, in *Physics of Ice Core Records 2*, edited by T. Hondoh., 2010b.

Levenberg, K.: A method for the solution of certain problems in least squares, *Q. Appl. Math.*, 2, 164–168, 1944.

Lipenkov, V. Y., Raynaud, D., Loutre, M. F. and Duval, P.: On the potential of coupling air content and O₂/N₂ from trapped air for establishing an ice core chronology tuned on local insolation, *Quat. Sci. Rev.*, 30(23), 3280–3289, 2011.

Lliboutry, L.: A critical review of analytical approximate solutions for steady state velocities and temperature in cold ice sheets, *Z Gletscherkd Glacialgeol*, 15(2), 135–148, 1979.

Louergue, L., Parrenin, F., Blunier, T., Barnola, J.-M., Spahni, R., Schilt, A., Raisbeck, G. and Chappellaz, J.: New constraints on the gas age-ice age difference along the {EPICA} ice cores, 0-50 kyr, *Clim Past*, 3(3), 527–540, 2007.

Louergue, L., Schilt, A., Spahni, R., Masson-Delmotte, V., Blunier, T., Lemieux, B., Barnola, J. M., Raynaud, D., Stocker, T. F. and Chappellaz, J.: Orbital and millennial-scale features of atmospheric CH₄ over the past 800,000 years, *Nature*, 453(7193), 383–386, 2008.

Marcott, S. A., Bauska, T. K., Buzert, C., Steig, E. J., Rosen, J. L., Cuffey, K. M., Fudge, T. J., Severinghaus, J. P., Ahn, J., Kalk, M. L. and others: Centennial-scale changes in the global carbon cycle during the last deglaciation, *Nature*, 514(7524), 616–619, 2014.

Marquardt, D. W.: An algorithm for least-squares estimation of nonlinear parameters, *J. Soc. Ind. Appl. Math.*, 11(2), 431–441, 1963.

Monnin, E., Indermühle, A., Dällenbach, A., Flückiger, J., Stauffer, B., Stocker, T. F., Raynaud, D. and Barnola, J.-M.: Atmospheric CO₂ concentrations over the last glacial termination, *Science*, 291(5501), 112–114, 2001.

Monnin, E., Steig, E. J., Siegenthaler, U., Kawamura, K., Schwander, J., Stauffer, B., Stocker, T. F., Morse, D. L., Barnola, J.-M., Bellier, B. and others: Evidence for substantial accumulation rate variability in Antarctica during the Holocene, through synchronization of CO₂ in the Taylor Dome, Dome C and DML ice cores, *Earth Planet. Sci. Lett.*, 224(1), 45–54, 2004.

Narcisi, B., Petit, J.-R. and Tiepolo, M.: A volcanic marker (92 ka) for dating deep east {A}ntarctic ice cores, *Quat Sci Rev*, 25, 2682–2687, 2006.

NEEM community Members: Eemian interglacial reconstructed from a Greenland folded ice core, *Nature*, 493(7433), 489–494, doi:10.1038/nature11789, 2013.

NorthGRIP project members: High-resolution record of Northern Hemisphere climate extending into the last interglacial period, *Nature*, 431, 147–151, 2004.

Parrenin, F., Barker, S., Blunier, T., Chappellaz, J., Jouzel, J., Landais, A., Masson-Delmotte, V., Schwander, J. and Veres, D.: On the gas-ice depth difference (Δ depth) along the EPICA Dome C ice core, *Clim Past*, 8(4), 1239–1255, doi:10.5194/cp-8-1239-2012, 2012a.

Parrenin, F., Barnola, J.-M., Beer, J., Blunier, T., Castellano, E., Chappellaz, J., Dreyfus, G., Fischer, H., Fujita, S. and Jouzel, J.: The EDC3 chronology for the EPICA Dome C ice core, *Clim. Past*, 3, 485–497, 2007a.

Parrenin, F., Dreyfus, G., Durand, G., Fujita, S., Gagliardini, O., Gillet, F., Jouzel, J., Kawamura, K., Lhomme, N., Masson-Delmotte, V., Ritz, C., Schwander, J., Shoji, H., Uemura, R., Watanabe, O. and Yoshida, N.: 1D ice flow modelling at EPICA Dome C and Dome Fuji, East Antarctica, *Clim Past*, 3, 243–259, 2007b.

Parrenin, F. and Hindmarsh, R. C. A.: Influence of a non-uniform velocity field on isochrone geometry along a steady flowline of an ice sheet, *J Glaciol*, 53(183), 612–622, 2007.

Parrenin, F., Hindmarsh, R. C. H. and Rémy, F.: Analytical solutions for the effect of topography, accumulation rate and lateral flow divergence on isochrone layer geometry, *J Glaciol*, 52(177), 191–202, 2006.

Parrenin, F., Jouzel, J., Waelbroeck, C., Ritz, C. and Barnola, J.-M.: Dating the Vostok ice core by an inverse method, *J Geophys Res*, 106(D23), 31,831–837,851, 2001.

Parrenin, F., Masson-Delmotte, V., Köhler, P., Raynaud, D., Paillard, D., Schwander, J., Barbante, C., Landais, A., Wegner, A. and Jouzel, J.: Synchronous change of atmospheric CO₂ and Antarctic temperature during the last deglacial warming, *Science*, 339(6123), 1060–1063, 2013.

Parrenin, F., Petit, J.-R., Masson-Delmotte, V., Wolff, E., Basile-Doelsch, I., Jouzel, J., Lipenkov, V., Rasmussen, S. O., Schwander, J., Severi, M., Udisti, R., Veres, D. and Vinther, B. M.: Volcanic synchronisation between the EPICA Dome C and Vostok ice cores (Antarctica) 0–145 kyr BP, *Clim Past*, 8(3), 1031–1045, doi:10.5194/cp-8-1031-2012, 2012b.

Parrenin, F., Rémy, F., Ritz, C., Siegert, M. and Jouzel, J.: New modelling of the Vostok ice flow line and implication for the glaciological chronology of the Vostok ice core, *J Geophys Res*, 109, D20102, doi:10.1029/2004JD004561, 2004.

Pedro, J. B., van Ommen, T. D., Rasmussen, S. O., Morgan, V. I., Chappellaz, J., Moy, A. D., Masson-Delmotte, V. and Delmotte, M.: The last deglaciation: timing the bipolar seesaw, *Clim Past*, 7(2), 671–683, doi:10.5194/cp-7-671-2011, 2011.

Petit, J. R., Jouzel, J., Raynaud, D., Barkov, N. I., Barnola, J.-M., Basile, I., Bender, M., Chappellaz, J., Devis, M., Delaygue, G., Delmotte, M., Kotlyakov, V. M., Legrand, M., Lipenkov, V. Y., Lorius, C., Pepin, L., Ritz, C., Saltzman, E. and Stievenard, M.: Climate and

atmospheric history of the past 420,000 years from the Vostok ice core, Antarctica, *Nature*, 399(6735), 429–436, 1999.

Raisbeck, G. M., Yiou, F., Bard, E., Dollfus, D., Jouzel, J. and Petit, J. R.: Absolute dating of the last 7000 years of the Vostok ice core using ^{10}Be , *Miner. Mag.*, 62A, 1228, 1998.

Raisbeck, G. M., Yiou, F., Cattani, O. and Jouzel, J.: ^{10}Be evidence for the Matuyama–Brunhes geomagnetic reversal in the EPICA Dome C ice core, *Nature*, 444(7115), 82–84, 2006.

Raisbeck, G. M., Yiou, F., Jouzel, J. and Stocker, T. F.: Direct north-south synchronization of abrupt climate change record in ice cores using Beryllium 10, *Clim Past*, 3(3), 541–547, 2007.

Rasmussen, S. O., Andersen, K. K., Svensson, A. M., Steffensen, J. P., Vinther, B. M., Clausen, H. B., Siggaard-Andersen, M.-L., Johnsen, S. J., Larsen, L. B., Dahl-Jensen, D., Bigler, M., Röthlisberger, R., Fischer, H., Goto-Azuma, K., Hansson, M. E. and Ruth, U.: A new {G}reenland ice core chronology for the last glacial termination, *J Geophys Res*, 111, D06102, doi:10.1029/2005JD006079, 2006.

Raynaud, D., Lipenkov, V., Lemieux-Dudon, B., Duval, P., Loutre, M.-F. and Lhomme, N.: The local insolation signature of air content in Antarctic ice. A new step toward an absolute dating of ice records, *Earth Planet Sci Lett*, 261(3-4), 337–349, 2007.

Röthlisberger, R., Mudelsee, M., Bigler, M., de Angelis, M., Fischer, H., Hansson, M., Lambert, F., Masson-Delmotte, V., Sime, L., Udisti, R. and Wolff, E. W.: The Southern Hemisphere at glacial terminations: insights from the Dome C ice core, *Clim Past*, 4(4), 345–356, doi:10.5194/cp-4-345-2008, 2008.

Schilt, A., Baumgartner, M., Blunier, T., Schwander, J., Spahni, R., Fischer, H. and Stocker, T. F.: Glacial–interglacial and millennial-scale variations in the atmospheric nitrous oxide concentration during the last 800,000 years, *Quat. Sci. Rev.*, 29(1), 182–192, 2010.

Schoenemann, S. W., Steig, E. J., Ding, Q., Markle, B. R. and Schauer, A. J.: Triple water-isotopologue record from WAIS Divide, Antarctica: Controls on glacial-interglacial changes in ^{17}O excess of precipitation, *J. Geophys. Res. Atmospheres*, 119(14), 8741–8763, 2014.

Schüpbach, S., Federer, U., Bigler, M., Fischer, H. and Stocker, T. F.: A refined TALDICE-1a age scale from 55 to 112 ka before present for the Talos Dome ice core based on high-resolution methane measurements, *Clim. Past*, 7(3), 1001–1009, 2011.

Schwander, J., Barnola, J.-M., Andrié, C., Leuenberger, M., Ludin, A., Raynaud, D. and Stauffer, B.: The age of the air in the firn and the ice at Summit, Greenland, *J. Geophys. Res. Atmospheres* 1984–2012, 98(D2), 2831–2838, 1993.

Seierstad, I. K., Abbott, P. M., Bigler, M., Blunier, T., Bourne, A. J., Brook, E., Buchardt, S. L., Buizert, C., Clausen, H. B., Cook, E. and others: Consistently dated records from the Greenland GRIP, GISP2 and NGRIP ice cores for the past 104 ka reveal regional millennial-scale $\delta^{18}\text{O}$ gradients with possible Heinrich event imprint, *Quat. Sci. Rev.*, 106, 29–46, 2014.

Severi, M., Castellano, E., Morganti, A., Udisti, R., Ruth, U., Fischer, H., Huybrechts, P., Wolff, E., Parrenin, F., Kaufmann, P., Lambert, F. and Steffensen, J. P.: Synchronisation of the

EDML1 and EDC3 timescales for the last 52 kyr by volcanic signature matching, *Clim Past*, 3, 367–374, 2007.

Severi, M., Udisti, R., Becagli, S., Stenni, B. and Traversi, R.: Volcanic synchronisation of the EPICA-DC and TALDICE ice cores for the last 42 kyr BP, *Clim Past*, 8(2), 509–517, doi:10.5194/cp-8-509-2012, 2012.

Sigl, M., McConnell, J. R., Toohey, M., Curran, M., Das, S. B., Edwards, R., Isaksson, E., Kawamura, K., Kipfstuhl, S., Krüger, K., Layman, L., Maselli, O. J., Motizuki, Y., Motoyama, H., Pasteris, D. R. and Severi, M.: Insights from Antarctica on volcanic forcing during the Common Era, *Nat. Clim. Change*, 4(8), 693–697, 2014.

Singer, B. S., Guillou, H., Jicha, B. R., Laj, C., Kissel, C., Beard, B. L. and Johnson, C. M.: $^{40}\text{Ar}/^{39}\text{Ar}$, K–Ar and ^{230}Th – ^{238}U dating of the Laschamp excursion: a radioisotopic tie-point for ice core and climate chronologies, *Earth Planet. Sci. Lett.*, 286(1-2), 80–88, 2009.

Stenni, B., Masson-Delmotte, V., Selmo, E., Oerter, H., Meyer, H., Röthlisberger, R., Jouzel, J., Cattani, O., Falourd, S., Fischer, H., Hoffmann, G., Iacumin, P., Johnsen, S. J., Minster, B. and Udisti, R.: The deuterium excess records of EPICA Dome C and Dronning Maud Land ice cores (East Antarctica), *Quat. Sci. Rev.*, 29(1-2), 146–159, doi:DOI: 10.1016/j.quascirev.2009.10.009, 2010.

Suwa, M. and Bender, M. L.: Chronology of the Vostok ice core constrained by O_2/N_2 ratios of occluded air, and its implication for the Vostok climate records, *Quat. Sci. Rev.*, 27(11), 1093–1106, 2008.

Svensson, A., Andersen, K. K., Bigler, M., Clausen, H. B., Dahl-Jensen, D., Davies, S. M., Johnsen, S. J., Muscheler, R., Parrenin, F., Rasmussen, S. O., Röthlisberger, R., Seierstad, I., Steffensen, J. P. and Vinther, B. M.: A 60 000 year Greenland stratigraphic ice core chronology, *Clim Past*, 4(1), 47–57, 2008.

Svensson, A., Bigler, M., Blunier, T., Clausen, H. B., Dahl-Jensen, D., Fischer, H., Fujita, S., Goto-Azuma, K., Johnsen, S. J. and Kawamura, K.: Direct linking of Greenland and Antarctic ice cores at the Toba eruption (74 ka BP), *Clim. Past*, 9(2), 749–766, 2013.

Tarantola, A.: Inverse problem theory and methods for model parameter estimation, Society for Industrial Mathematics., 2005.

Udisti, R., Becagli, S., Castellano, E., Delmonte, B., Jouzel, J., Petit, J.-R., Schwander, J., Stenni, B. and Wolff, E. W.: Stratigraphic correlations between the EPICA-Dome C and Vostok ice cores showing the relative variations of snow accumulation over the past 45 kyr, *J Geophys Res*, 109(D8), D08101, doi:10.1029/2003JD004180, 2004.

Veres, D., Bazin, L., Landais, A., Toyé Mahamadou Kele, H., Lemieux-Dudon, B., Parrenin, F., Martinerie, P., Blayo, E., Blunier, T., Capron, E., Chappellaz, J., Rasmussen, S. O., Severi, M., Svensson, A., Vinther, B. and Wolff, E. W.: The Antarctic ice core chronology (AICC2012): an optimized multi-parameter and multi-site dating approach for the last 120 thousand years, *Clim Past*, 9(4), 1733–1748, doi:10.5194/cp-9-1733-2013, 2013.

Vinther, B., Clausen, H., Kipfstuhl, S., Fischer, H., Bigler, M., Oerter, H., Wegner, A., Wilhelms, F., Sevri, M., Udisti, R. and others: A stratigraphic Antarctic chronology covering

the past 16700 years in the EPICA deep ice core from Dronning Maud Land, preparation., 2013.

WAIS Divide Project Members: Onset of deglacial warming in West Antarctica driven by local orbital forcing, *Nature*, 500(7463), 440–444, 2013.

Winkler, R., Landais, A., Sodemann, H., Dümbgen, L., Prié, F., Masson-Delmotte, V., Stenni, B. and Jouzel, J.: Deglaciation records of ^{17}O -excess in East Antarctica: reliable reconstruction of oceanic normalized relative humidity from coastal sites, *Clim Past*, 8(1), 1–16, doi:10.5194/cp-8-1-2012, 2012.

Winstrup, M., Svensson, A. M., Rasmussen, S. O., Winther, O., Steig, E. J. and Axelrod, A. E.: An automated approach for annual layer counting in ice cores, *Clim Past*, 8(6), 1881–1895, doi:10.5194/cp-8-1881-2012, 2012.

Wolff, E. W., Fischer, H., Fundel, F., Ruth, U., Twarloh, B., Littot, G. C., Mulvaney, R., Röhlisberger, R., de Angelis, M., Boutron, C. F., Hansson, M., Jonsell, U., Hutterli, M. A., Lambert, F., Kaufmann, P., Stauffer, B., Stocker, T. F., Steffensen, J. P., Bigler, M., Siggaard-Andersen, M. L., Udisti, R., Becagli, S., Castellano, E., Severi, M., Wagenbach, D., Barbante, C., Gabrielli, P. and Gaspari, V.: Southern Ocean sea-ice extent, productivity and iron flux over the past eight glacial cycles, *Nature*, 440, 491–496, 2006.

Yiou, F., Raisbeck, G. M., Baumgartner, S., Beer, J., Hammer, C., Johnsen, J., Jouzel, J., Kubik, P. W., Lestringuez, J., Stievenard, M., Suter, M. and Yiou, P.: Beryllium 10 in the Greenland Ice Core Project ice core at Summit, Greenland, *J Geophys Res*, 102, 783,794, 1997.

Symbol	Definition
k, m	Indices of ice cores
z_k	Depth
χ_k	Ice age
D_k	Relative density
a_k	Accumulation rate
τ_k	Thinning function
Δd_k	Δdepth, depth shift between synchronous ice and air events
l_k	Lock-In Depth of air bubbles
D^{firm}_k	Average relative density between surface and Lock-In Depth
a^b_k	Prior accumulation rate
l^b_k	Prior Lock-In Depth of air bubbles
τ^b_k	Prior thinning function
c^a_k	Accumulation correction function
c^l_k	Lock-In Depth correction function
c^τ_k	Thinning correction function
$z_{k,i}$	Discretized depth z_k for the solving the age equations
$t^a_{k,i}$	Discretized time for the accumulation correction function
$t^l_{k,i}$	Discretized time for the Lock-In-Depth correction function
$z^\tau_{k,i}$	Discretized depth for the thinning correction function
C^a_k	Accumulation correction vector
C^l_k	Lock-In Depth correction vector
C^τ_k	Thinning correction vector
X	Model input variables vector
L	Likelihood function
J	Cost function

J_k	Cost function term for ice core k
$J_{k,m}$	Cost function term for ice cores couple (k,m)
J^a_k	Accumulation prior cost term
J^l_k	Lock-In Depth prior cost term
J^r_k	Thinning prior cost term
J^{ih}_k	Ice dated horizons cost term
J^{ah}_k	Air dated horizons cost term
J^{ii}_k	Ice intervals with known durations cost term
J^{ai}_k	Air intervals with known durations cost term
$J^{\Delta d}_k$	Δ depth cost term
$J^{ii}_{k,m}$	Ice-ice stratigraphic links cost term
$J^{aa}_{k,m}$	Air-air stratigraphic links cost term
$J^{ia}_{k,m}$	Ice-air stratigraphic links cost term
$J^{ai}_{k,m}$	Air-ice stratigraphic links cost term
\mathbf{P}^a_k	Accumulation prior correlation matrix
\mathbf{P}^l_k	Lock-In-Depth prior correlation matrix
\mathbf{P}^r_k	Thinning prior correlation matrix
R^a_k	Accumulation residual vector
R^l_k	Lock-In-Depth residual vector
R^r_k	Thinning residual vector
$(\sigma^a_{k,i})_i$	Accumulation prior standard deviation vector
$(\sigma^l_{k,i})_i$	Lock-In-Depth prior standard deviation vector
$(\sigma^r_{k,i})_i$	Thinning prior standard deviation vector
X^{opt}	Optimized model input variables vector
\mathbf{C}^X	<i>A posteriori</i> covariance matrix of the model input variable
\mathbf{G}'	Model Jacobian

\mathbf{C}^G	<i>A posteriori</i> covariance matrix of the model
----------------	--

Table 1: List of symbols

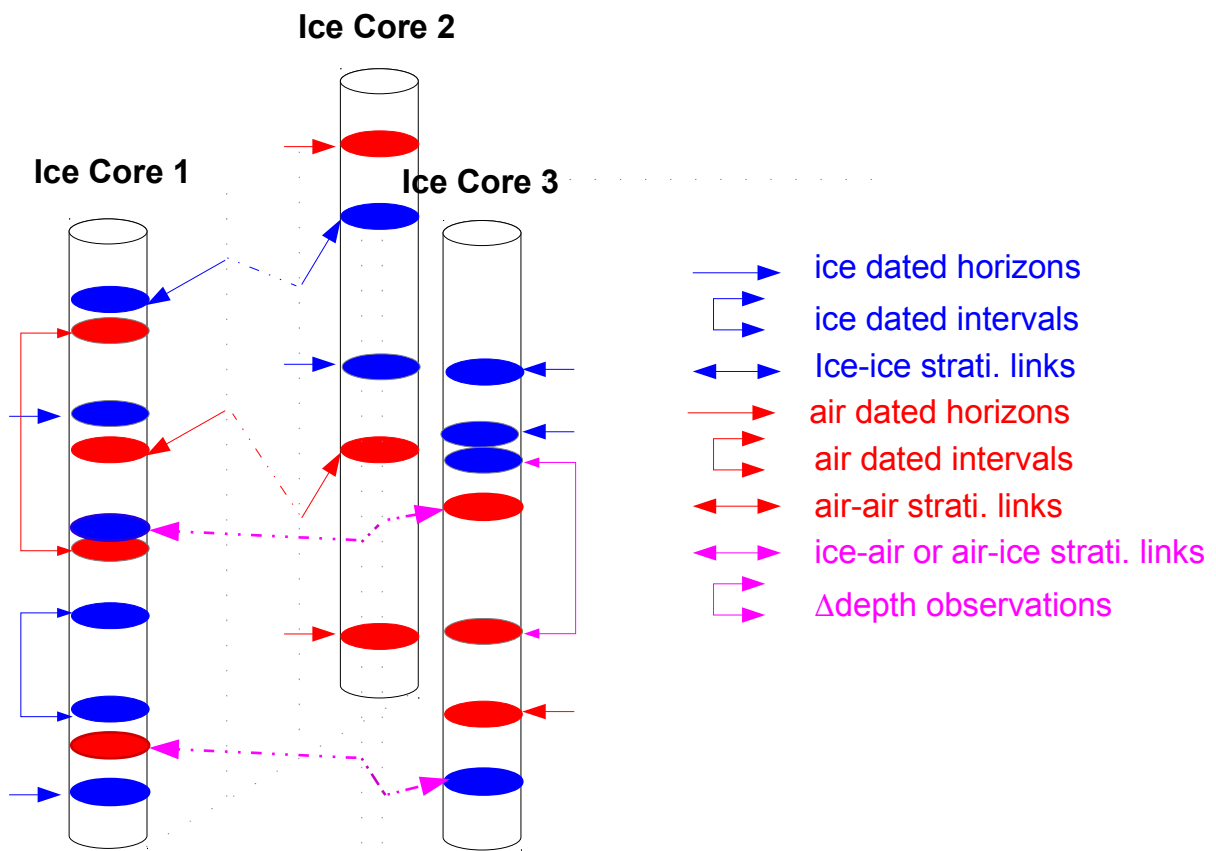


Figure 1: Scheme illustrating the different kinds of observations used to constrain the chronologies of the ice cores in the IceChrono model.

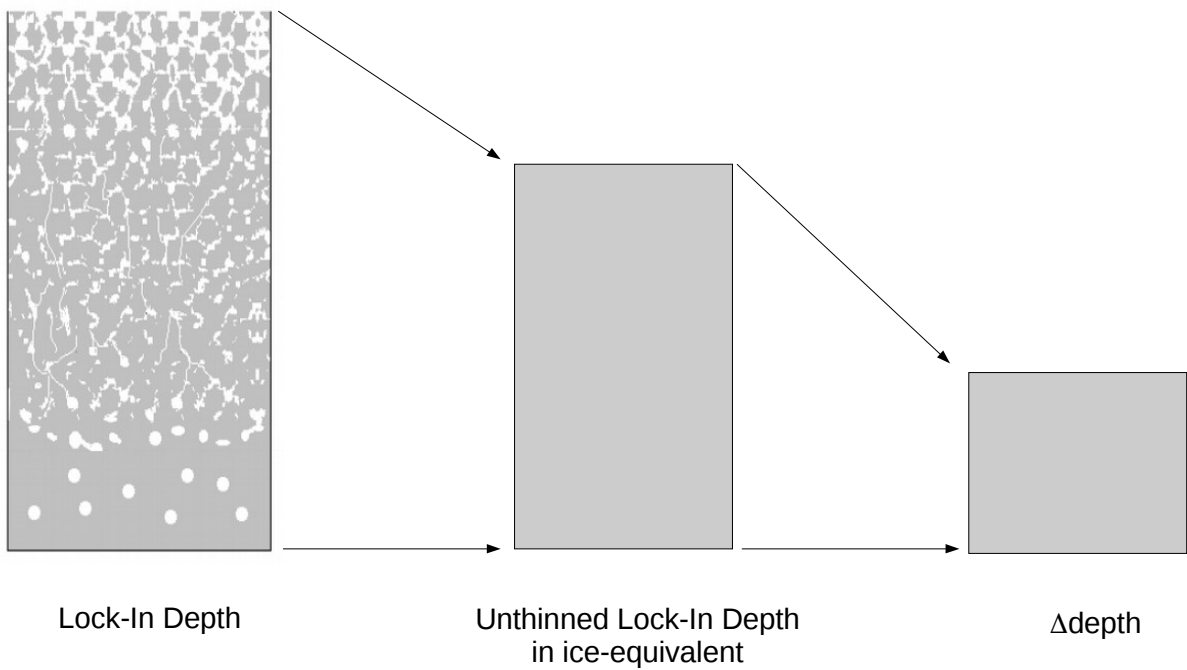


Figure 2: Scheme of different representations of a firn column. **(Left)** When the firn column is at surface, its height is equal to the Lock-In Depth. **(Middle)** If one virtually converts the firn column into cumulated ice-equivalent accumulations, one gets the Unthinned Lock-In Depth in Ice Equivalent (ULIDIE). **(Right)** When the firn column is buried down into the ice sheet and encounters vertical thinning, its height decreases to Δ depth.

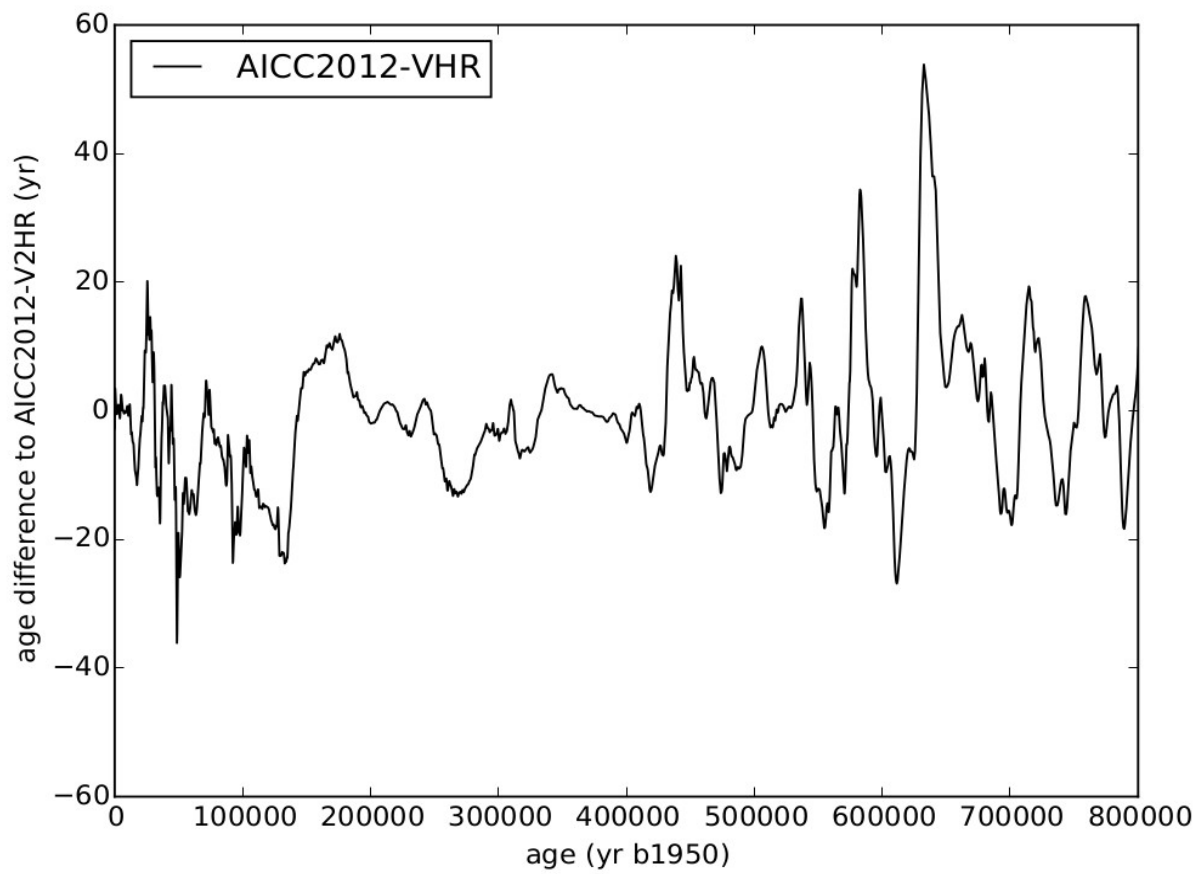


Figure 3: Sensitivity of the AICC2012-like experiment to a change of resolution of the correction functions. The black line is the age difference between the AICC2012-V2HR and AICC2012-VHR experiments (see text).

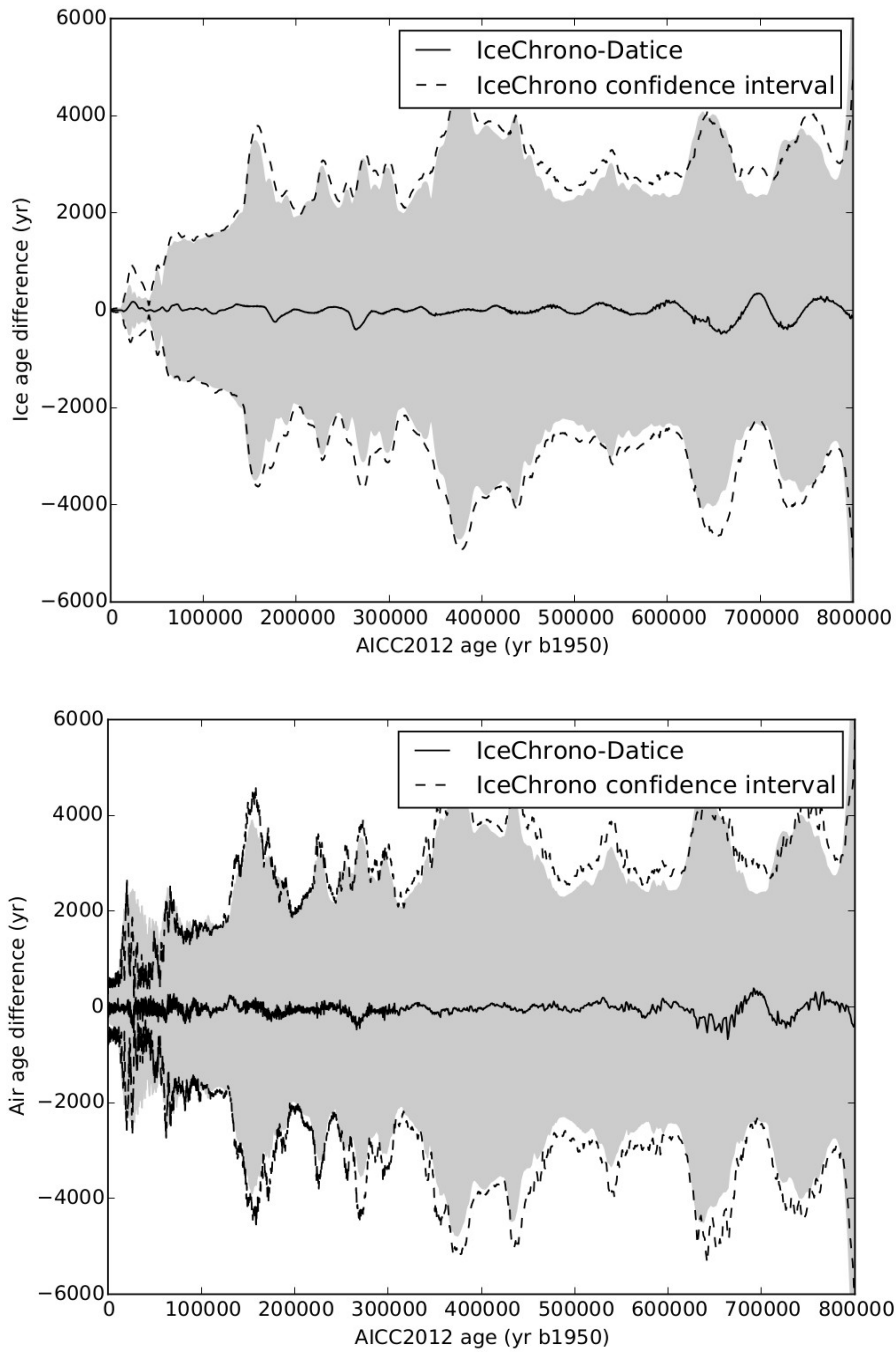


Figure 4: Comparison of IceChrono and Datice chronologies of the EDC ice core in the AICC2012 experiment. IceChrono is the black plain line and its standard deviation is the black dashed line. AICC2012 standard deviation is represented by the grey area. **(top)** Ice chronologies. **(bottom)** Air chronologies.

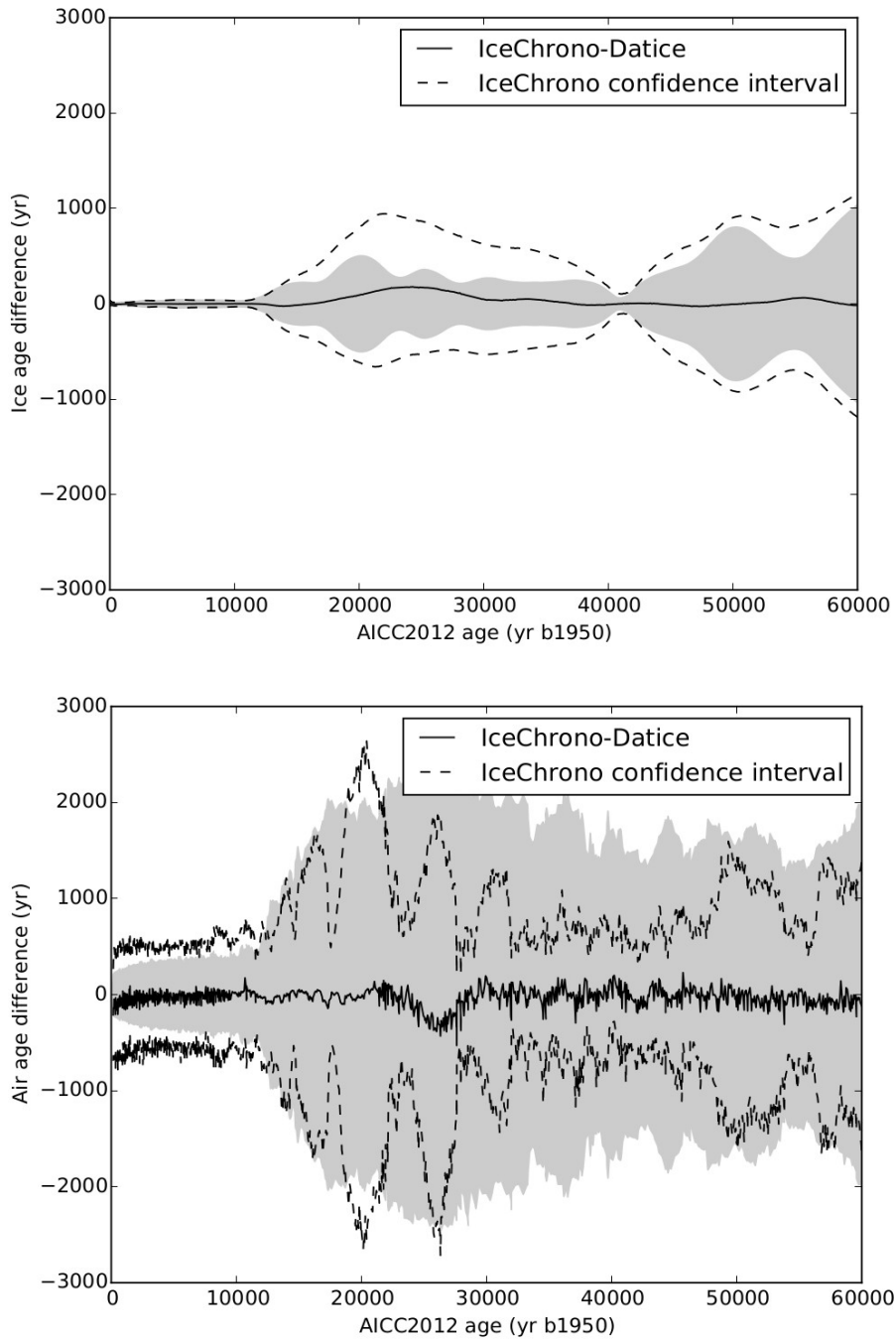


Figure 5: Comparison of IceChrono and Datice chronologies of the EDC ice core in the AICC2012 experiment, for the last 60 kyr. IceChrono is the black plain line and its standard deviation is the black dashed line. AICC2012 standard deviation is represented by the grey area. **(top)** Ice chronologies. **(bottom)** Air chronologies.

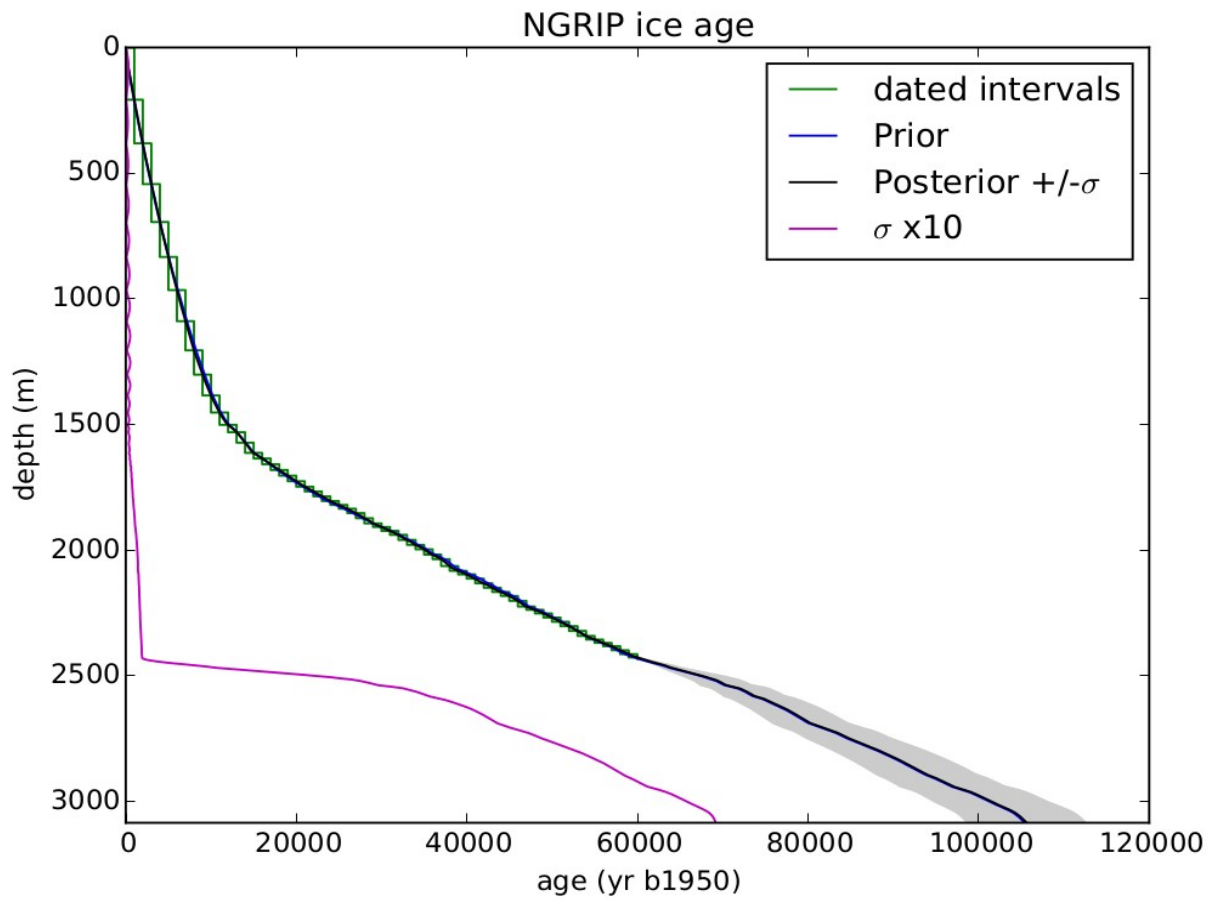


Figure 6: Experiment test-ice-intervals-with-known-durations. NGRIP prior (blue) and posterior (black) chronologies and the posterior confidence interval (grey area) when using independent 1 kyr long intervals with known durations from the GICC05 layer counted time scale (green rectangles, Svensson et al., 2008). The 1σ uncertainty of the posterior time scale is also shown on the left (pink). This figure is automatically produced by IceChrono1.

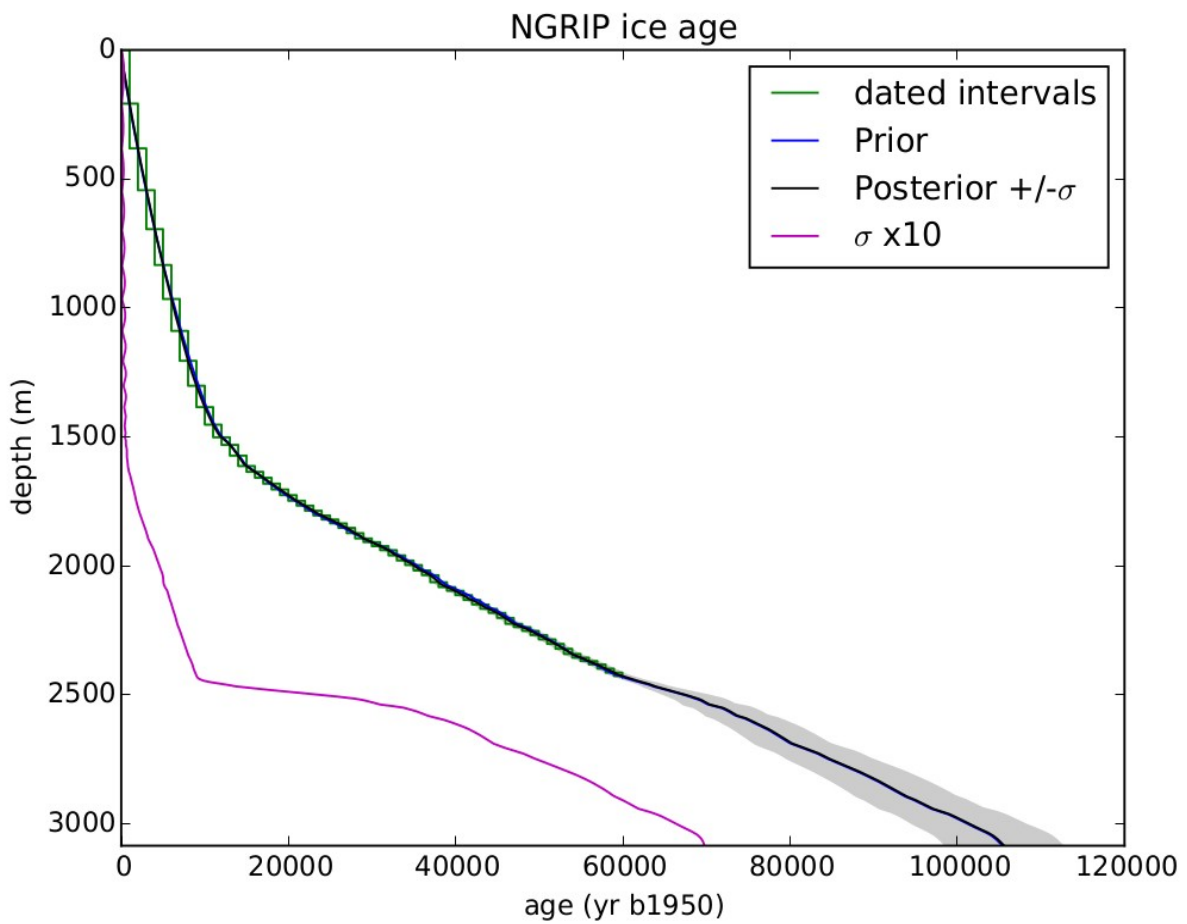


Figure 7: Experiment test-ice-intervals-with-known-durations-with-correlation. NGRIP prior (blue) and posterior (black) chronologies and the posterior confidence interval (grey area) when using correlated 1 kyr long intervals with known durations from the GICC05 layer counted time scale (green rectangles, Svensson et al., 2008). The 1σ uncertainty of the posterior time scale is also shown on the left (pink). This figure is automatically produced by IceChrono1.

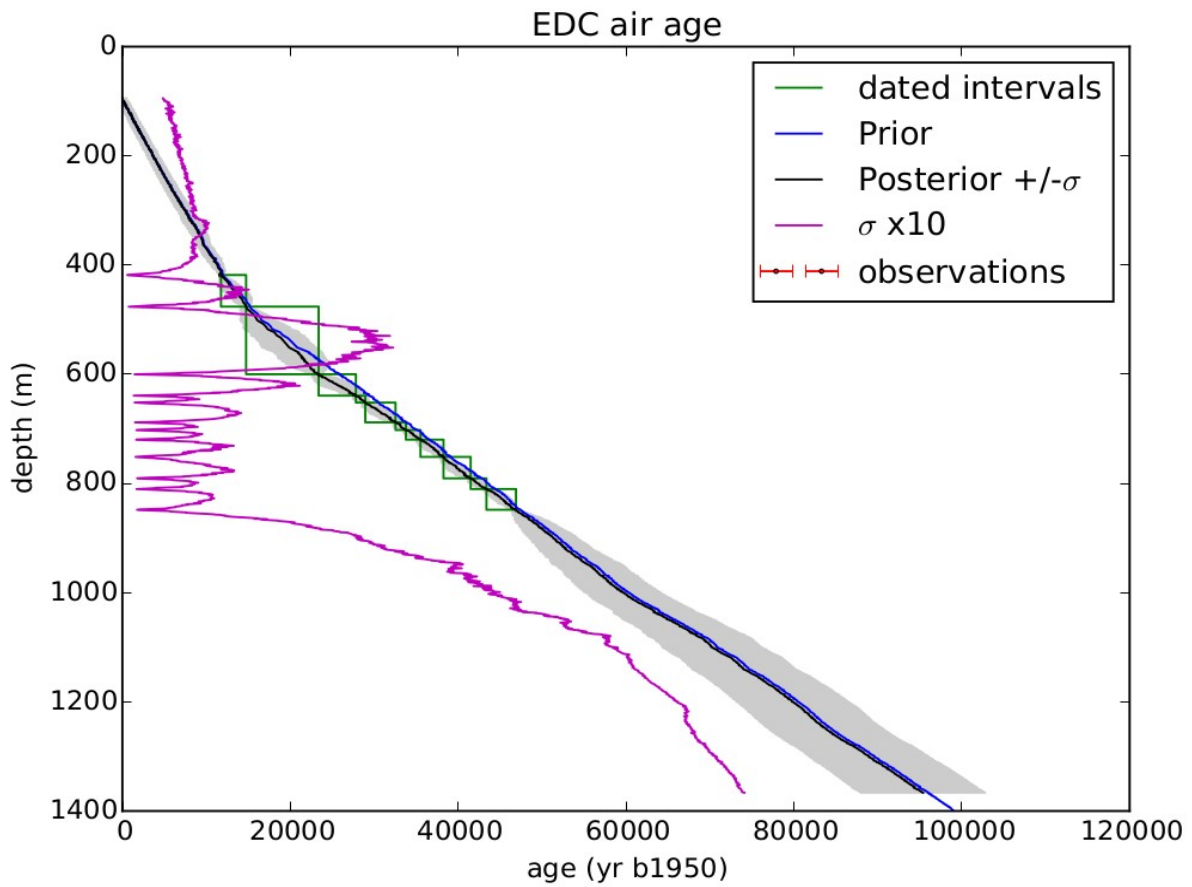


Figure 8: Experiment test-air-intervals-with-known-durations. EDC prior (blue) and posterior (black) chronologies and the posterior confidence interval (grey area) when using independent CH_4 intervals with known durations from the GICC05 layer counted time scale (green rectangles, Svensson et al., 2008). The 1σ uncertainty of the posterior time scale is also shown on the left (pink). This figure is automatically produced by IceChrono1.

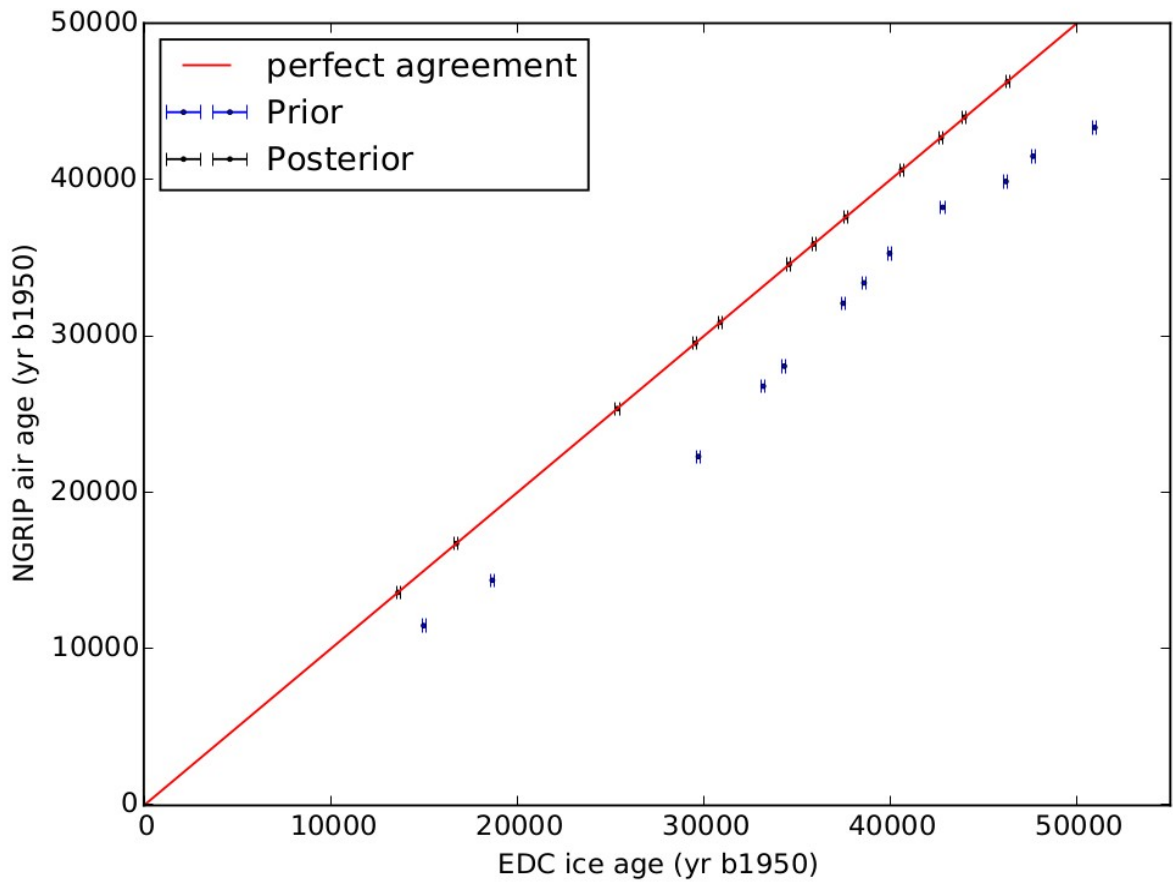


Figure 9: Experiment test-mix-strati. NGRIP air age vs EDC ice age for the prior (blue) and posterior (black) scenarios for the stratigraphic observations. The 1:1 perfect agreement line (red) is shown for comparison. This figure is automatically produced by IceChrono1.